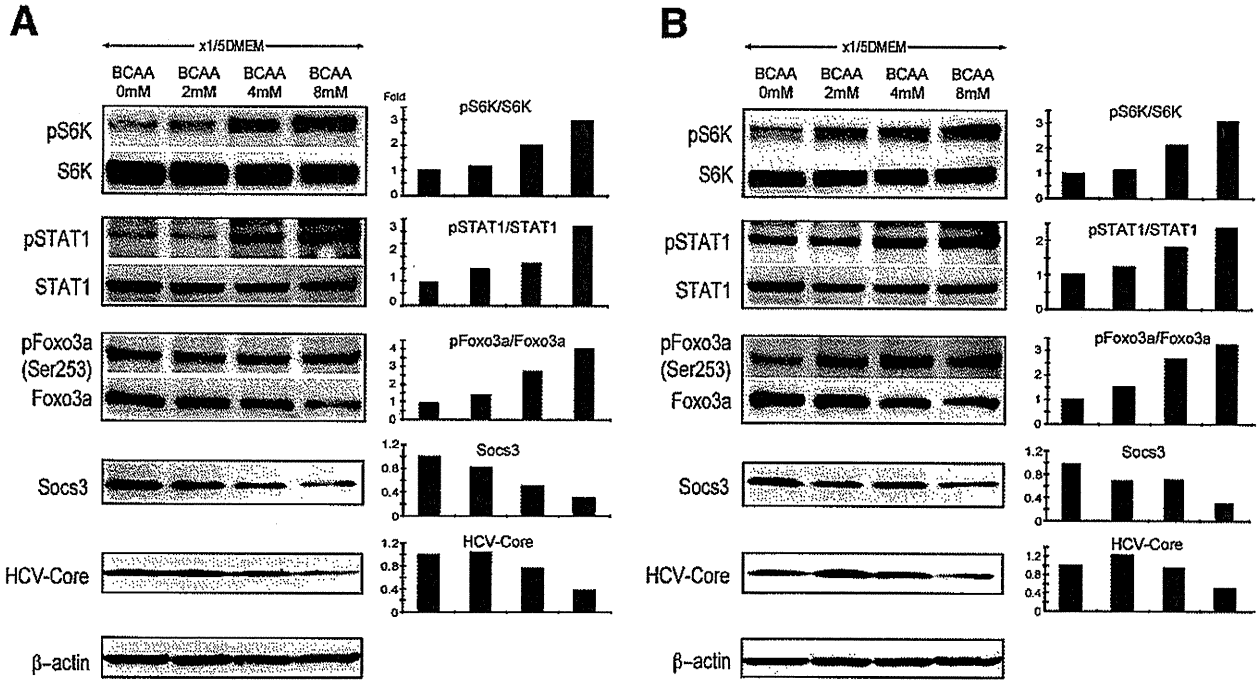

Figure 6. Expression of S6K, STAT1, Foxo3a, Socs3, and HCV core in H77S.3/GLuc2A-transfected Huh-7.5 cells or continuously JFH-1–infecting Huh-7 cells supplemented with BCAA.

ment of patients with liver malnutrition and impaired mTORC1 signaling would lead to reduced induction of ISGs. Importantly, BCAA was able to restore impaired IFN signaling through increased binding of ISGF3γ to its targets (Figure 2*D–F*).

Besides cross-talk of mTORC1 and IFN signaling, we revealed that Foxo3a also is involved in the IFN inhibitory pathway. In low-amino-acid medium, expression of pFoxo3a (ser253) was decreased substantially whereas that of Socs3 was increased. A decreased pFoxo3a/Foxo3a ratio indicates nuclear accumulation of Foxo3a before activation of its target genes, and this was confirmed by immunofluorescent staining (Figure 3*C*). The expression of Foxo3a was significantly positively correlated with that of Socs3 in CH-C liver (Figure 3*F*). These findings prompted us to identify a putative FBE in the Socs3 promoter region (Figure 4*A*). In fact, Socs3 promoter reporter activity was activated by overexpression of Foxo3a, and mutation of FBE impaired Foxo3a-dependent Socs3 promoter activation. Conversely, induction of Socs3 was not observed when expression of Foxo3a was knocked down by siRNA in low-amino-acid medium. Socs3 induction in low-amino-acid medium was owing to increased binding of Foxo3a to the FBE, which was confirmed by ChIP (Figure 4*D*). Therefore, in addition to impaired mTORC1 signaling, the Foxo3a-mediated Socs3 IFN inhibitory pathway might be involved in impaired IFN signaling in patients with liver malnutrition (Figure 4*E*).

Finally, we examined whether BCAA could restore impaired IFN signaling and inhibit HCV replication in cells under conditions of malnutrition. Importantly, BCAA could repress replication of the recombinant genotype 1a-derived HCV, H77S.3/GLuc2A, in a dose-dependent manner (Figure 5*A*). H77S.3/GLuc2A RNA produces infectious virus[14] and, therefore, the results indicate that BCAA might act on a naive HCV infection. Moreover, BCAA inhibited JFH-1–infected Huh-7 cells in which JFH-1 continuously was infecting in a dose-dependent manner. These results indicate that BCAA had an inhibitory effect on either naive or persistent HCV infection irrespective of genotypes (1a and 2a). Consistent with these results, BCAA induced the expression of pSTAT1 and Mx protein in a dose-dependent manner, and repressed Socs3 expression through increasing the ratio of pFoxo3a (ser243) to Foxo3a in a dose-dependent manner (Figures 5 and 6). Therefore, BCAA potentially could restore impaired IFN signaling and inhibit HCV replication in a CH-C state of malnutrition.

In conclusion, we addressed the clinical significance of the nutritional state of the liver on the treatment response of Peg-IFN and RBV combination therapy for CH-C. Although further studies are required to fully define the precise mechanisms underlying mTOR and IFN signaling, we showed that plasma values of Fischer's ratio are a useful nutritional parameter associated with treatment response. Fischer's ratio reflects mTORC1 signaling in the liver, which is correlated with IFN signaling and related to Socs3 IFN inhibitory signaling through Foxo3a. The potential usefulness of BCAA for the augmentation of IFN signaling could suggest a new therapeutic application for advanced-stage CH-C.

Supplementary Material

Note: To access the supplementary material accompanying this article, visit the online version of *Gastroenterology* at www.gastrojournal.org, and at doi: 10.1053/j.gastro.2011.03.051.

Appendix A

The Hokuriku Liver Study Group is composed of the following members: Drs Takashi Kagaya, Kuniaki Arai, Kaheita Kakinoki, Kazunori Kawaguchi, Hajime Takatori, and Hajime Sunakosaka (Department of Gastroenterology, Kanazawa University Graduate School of Medicine, Kanazawa, Japan); Drs Touru Nakahama and Shinji Kamiyamamoto (Kurobe City Hospital, Kurobe, Toyama, Japan); Dr Yasuhiro Takemori (Toyama Rosai Hospital, Uozu, Toyama, Japan); Dr Hikaru Oguri (Koseiren Namerikawa Hospital, Namerikawa, Toyama, Japan); Drs Yatsugi Noda and Hidero Ogino (Toyama Prefectural Central Hospital, Toyama, Japan); Drs Yoshinobu Hinoue and Keiji Minouchi (Toyama City Hospital, Toyama, Japan); Dr Nobuyuki Hirai (Koseiren Takaoka Hospital, Takaoka, Toyama, Japan); Drs Tatsuho Sugimoto and Koji Adachi (Tonami General Hospital, Tonam, Toyama, Japan); Dr Yuichi Nakamura (Noto General Hospital, Nanao, Ishikawa, Japan); Drs Masashi Unoura and Ryuhei Nishino (Public Hakui Hospital, Hakui, Ishikawa, Japan); Drs Hideo Morimoto and Hajime Ohta (National Hospital Organization Kanazawa Medical Center, Kanazawa, Ishikawa, Japan); Dr Hirokazu Tsuji (Kanazawa Municipal Hospital, Kanazawa, Ishikawa, Japan); Drs Akira Iwata and Shuichi Terasaki (Kanazawa Red Cross Hospital, Kanazawa, Ishikawa, Japan); Drs Tokio Wakabayashi and Yukihiro Shirota (Saiseikai Kanazawa Hospital, Kanazawa, Ishikawa, Japan); Drs Takeshi Urabe and Hiroshi Kawai (Public Central Hospital of Matto Ishikawa, Hakusan, Ishikawa, Japan); Dr Yasutsugu Mizuno (Nomi Municipal Hospital, Nomi, Ishikawa, Japan); Dr Shoni Kameda (Komatsu Municipal Hospital, Komatsu Ishikawa, Japan); Drs Hirotoshi Miyamori and Uichiro Fuchizaki (Keiju Medical Center, Nanao, Ishikawa, Japan); Dr Haruhiko Shyugo (Kanazawa Arimatsu Hospital, Kanazawa, Ishikawa, Japan); Dr Hideki Osaka (Yawata Medical Center, Komatsu, Ishikawa, Japan); Dr Eiki Matsushita (Kahoku Central Hospital, Tsubata, Ishikawa, Japan); Dr Yasuhiro Katou (Katou Hospital, Komatsu, Ishikawa, Japan); Drs Nobuyoshi Tanaka and Kazuo Notsumata (Fukuiken Saiseikai Hospital, Fukui, Japan); Dr Mikio Kumagai (Kumagai Clinic, Tsuruga, Fukui, Japan); and Dr Manabu Yoneshima (Municipal Tsuruga Hospital, Tsuruga, Fukui, Japan).

References

1. Fried MW, Shiffman ML, Reddy KR, et al. Peginterferon alfa-2a plus ribavirin for chronic hepatitis C virus infection. N Engl J Med 2002;347:975–982.
2. Tanaka Y, Nishida N, Sugiyama M, et al. Genome-wide association of IL28B with response to pegylated interferon-alpha and ribavirin therapy for chronic hepatitis C. Nat Genet 2009;41:1105–1109.
3. Ge D, Fellay J, Thompson AJ, et al. Genetic variation in IL28B predicts hepatitis C treatment-induced viral clearance. Nature 2009;461:399–401.
4. Honda M, Sakai A, Yamashita T, et al. Hepatic ISG expression is associated with genetic variation in interleukin 28B and the outcome of IFN therapy for chronic hepatitis C. Gastroenterology 2010;139:499–509.
5. Thompson AJ, Muir AJ, Sulkowski MS, et al. Interleukin-28B polymorphism improves viral kinetics and is the strongest pretreatment predictor of sustained virologic response in genotype 1 hepatitis C virus. Gastroenterology 2010;139:120–129 e18.
6. Nishitani S, Ijichi C, Takehana K, et al. Pharmacological activities of branched-chain amino acids: specificity of tissue and signal transduction. Biochem Biophys Res Commun 2004;313:387–389.
7. Matsumura T, Morinaga Y, Fujitani S, et al. Oral administration of branched-chain amino acids activates the mTOR signal in cirrhotic rat liver. Hepatol Res 2005;33:27–32.
8. Kim DH, Sarbassov DD, Ali SM, et al. mTOR interacts with raptor to form a nutrient-sensitive complex that signals to the cell growth machinery. Cell 2002;110:163–175.
9. Colina R, Costa-Mattioli M, Dowling RJ, et al. Translational control of the innate immune response through IRF-7. Nature 2008;452:323–328.
10. Kaur S, Lal L, Sassano A, et al. Regulatory effects of mammalian target of rapamycin-activated pathways in type I and II interferon signaling. J Biol Chem 2007;282:1757–1768.
11. Shimbo K, Kubo S, Harada Y, et al. Automated precolumn derivatization system for analyzing physiological amino acids by liquid chromatography/mass spectrometry. Biomed Chromatogr 2009;24:683–691.
12. Shirasaki T, Honda M, Mizuno H, et al. La protein required for internal ribosome entry site-directed translation is a potential therapeutic target for hepatitis C virus replication. J Infect Dis 2010;202:75–85.
13. Yi M, Villanueva RA, Thomas DL, et al. Production of infectious genotype 1a hepatitis C virus (Hutchinson strain) in cultured human hepatoma cells. Proc Natl Acad Sci U S A 2006;103:2310–2315.
14. Shimakami T, Welsch C, Yamane D, et al. Protease inhibitor-resistant hepatitis C virus mutants with reduced fitness from impaired production of infectious virus. Gastroenterology 2011;140:667–675.
15. Eden A, Simchen G, Benvenisty N. Two yeast homologs of ECA39, a target for c-Myc regulation, code for cytosolic and mitochondrial branched-chain amino acid aminotransferases. J Biol Chem 1996;271:20242–2045.
16. Dowling RJ, Topisirovic I, Alain T, et al. mTORC1-mediated cell proliferation, but not cell growth, controlled by the 4E-BPs. Science 2010;328:1172–1176.
17. Teleman AA, Hietakangas V, Sayadian AC, et al. Nutritional control of protein biosynthetic capacity by insulin via Myc in Drosophila. Cell Metab 2008;7:21–32.
18. Zhang X, Gan L, Pan H, et al. Phosphorylation of serine 256 suppresses transactivation by FKHR (FOX01) by multiple mechanisms. Direct and indirect effects on nuclear/cytoplasmic shuttling and DNA binding. J Biol Chem 2002;277:45276–45284.
19. Farinati F, Cardin R, Bortolami M, et al. Oxidative damage, pro-inflammatory cytokines, TGF-alpha and c-myc in chronic HCV-related hepatitis and cirrhosis. World J Gastroenterol 2006;12:2065–2069.

Received October 19, 2010. Accepted March 18, 2011.

Reprint requests

Address requests for reprints to: Shuchi Kaneko, MD, PhD, Department of Gastroenterology, Graduate School of Medicine, Kanazawa University, Takara-Machi 13-1, Kanazawa 920-8641, Japan. e-mail: skaneko@m-kanazawa.jp; e-mail: fax: (81) 76-234-4250.

Acknowledgments

Participating investigators from the Hokuriku Liver Study Group are listed in Appendix A.

The authors thank Mina Nishiyama and Yuki Hatayama for excellent technical assistance.

Conflicts of interest

The authors disclose no conflicts.

Supplementary Materials and Methods

Plasma Amino Acid Analysis

Plasma sample amino acid concentrations were measured by high-performance liquid chromatography–electrospray ionization–mass spectrometry followed by derivatization.[1] An MSQ Plus LC/MS system (Thermo Fischer Scientific, Waltham, MA) equipped with an electrospray ionization source was used in positive ionization mode for selected ion monitoring. Xcalibur version 1.4 SR1 software (Thermo Fischer Scientific, Yokohama, Japan) was used for data collection and processing. The high-performance liquid chromatography separation system consisted of an L-2100 pump, L-2200 autosampler, and L-2300 column oven (Hitachi High-Technologies Corporation, Tokyo, Japan). A Wakosil-II 3C8-100HG column (100, 2.1, 3 mm; Wako Pure Chemical Industries, Osaka, Japan) was used for the separation, and the mobile phase consisted of eluent A (25-mmol/L ammonium formate in water, pH 6.0) and eluent B (water:acetonitrile = 40:60).

Western Blotting

The expression of HCV core protein, Socs3, Foxo3a, phospho-Foxo3a (Ser253) (pFoxo3a), STAT1, pSTAT1 (Tyr701), S6K, pS6K, p-mTOR (Ser2448), Raptor, and β-actin were evaluated with mouse anti-core (Affinity BioReagents, Golden, CO), mouse anti-Socs3 (Santa Cruz Biotechnology, Santa Cruz, CA), rabbit anti-Foxo3a, rabbit anti-β-actin (Sigma-Aldrich, St Louis, MO), rabbit anti-phospho-Foxo3a (Ser253), rabbit anti-STAT1, rabbit anti-p-STAT1 (Tyr701), rabbit anti-p70 S6K, rabbit anti-pS6K, rabbit anti-p-mTOR (Ser2448), and rabbit anti-Raptor (Cell Signaling Technology, Beverly, MA), respectively. Densitometric analysis was conducted directly on the blotted membrane using a charge coupled device camera system (LAS-3000 Mini; Fujifilm, Tokyo, Japan) and Scion Image software (Frederick, MD).

Primer Sequences for PCR and siRNA

Primer sequences for PCR and siRNA were as follows: 2′5′OAS: forward 5′- CTC AGA AAT ACC CCA GCC AAA TC-3′, reverse 5′-GTG GTG AGA GGA CTG AGG AA-3′; Socs3: forward 5′-TAC CAC CTG AGT CTC CAG CTT CTC-3′, reverse 5′-CCT GGC AGT TCT CAT TAG TTC AGC ATT C-3′; Foxo3a: forward 5′-TGC TGT ATG CAA GAA CTT TCC AGT AGC AG-3′, reverse 5′-ACT CTA GCC CCC ATG CTA CTA GTG-3′; glyceraldehyde-3-phosphate dehydrogenase: forward 5′-GAA GGT GAA GGT CGG AGT-3′, reverse 5′-GAA GAT GGT GAT GGG ATT TC-3′, siFoxo3a (SASI_Hs01_00119127; Sigma) sense: 5′-GAA UGA UGG GCU GAC UGA AdTdT-3′, antisense: 5′-UUC AGU CAG CCC AUC AUU CdTdT-3′. Small interfering Raptor was purchased as part of KIAA1303 siGENOME SMART pool siRNA reagents from Dharmacon, Inc (Lafayette, CO).

Construction of ISRE-Luc Reporter and FBEmut-luc Reporter Plasmids

Oligonucleotides containing the ISRE tandem repeat sequence (sense 5′-TCG AGA ACT GAA ACT GAA ACT GAA ACT GAA ACT GAA ACT GAA ACT GAA ACT GAA A-3′, antisense 5′-AGC TTT TCA GTT TCA GTT TCA GTT TCA GTT TCA GTT TCA GTT TCA GTT TCA GTT C-3′, consensus 5′-GAA Ann GAA ACT-3′) were annealed, and integrated into Xho I and Hind III sites of the pGL4.23 luciferase vector (Promega). The human Socs3 promoter region (-109/+217) was amplified by genomic PCR using specific primers (forward, 5′-TGC TGC GAG TAG TGA CTA AAC ATT ACA AG-3′ and reverse, 5′-CCG TGA AGT CCA CAA AGG AGC CTT C-3′) and cloned into the EcoR V site of the pGL4.10-luc2 reporter vector (Promega). The Socs3 FBE mutant reporter vector was created by substituting 2 adenines in the putative FBE with guanines (wild-type sequence 5′-CTAAACA-3′, mutated sequence 5′-CTGAGCA-3′).

ChIP Assay

For the ChIP assay using the anti-ISGF3γ antibody, 1×10^6 Huh-7 cells were treated with IFN-alfa (0 or 100 U/mL) and BCAA (2 mmol/L) in low-amino-acid medium for 6 hours. For ChIP using the anti-Foxo3a antibody, 1×10^6 Huh-7 cells were cultured in low-amino-acid medium for 24 hours.

Cells were cross-linked with 1% formaldehyde in PBS for 10 minutes at 37°C, and the reaction was stopped with 250 mmol/L glycine for 10 minutes. Cells were suspended in sodium dodecyl sulfate–lysis buffer (1% sodium dodecyl sulfate, 10 mmol/L ethylenediaminetetraacetic acid [EDTA], 50 mmol/L Tris-HCl [pH 8.1]), complete protease inhibitor cocktail (Roche Applied Science), and incubated for 30 minutes at 10°C. Cell lysate was sonicated with Bioruptor (Cosmo Bio, Tokyo, Japan) to obtain chromatin fragments and diluted 10-fold in ChIP dilution buffer (0.01% sodium dodecyl sulfate, 1.1% Triton-X 100, 1.2 mmol/L EDTA, 16.7 mmol/L Tris-HCl [pH 8.1], 150 mmol/L NaCl, complete protease inhibitor cocktail). Chromatin fragments were incubated with 2 μg ISGF3γ antibody (Santa Cruz Biotechnology), 2 μg Foxo3a antibody (H-144; Santa Cruz Biotechnology), or normal rabbit immunoglobulin G for 18 hours at 4°C. Dynabeads (30 μL) protein G (Invitrogen) was added and incubated for 1 hour at 4°C. The beads were washed with low-salt-wash buffer (0.1% sodium dodecyl sulfate, 1% Triton-X 100, 2.0 mmol/L EDTA, 20 mmol/L Tris-HCl [pH 8.1], 150 mmol/L NaCl), high-salt-wash buffer (0.1% sodium dodecyl sulfate, 1% Triton-X 100, 2.0 mmol/L EDTA, 20 mmol/L Tris-HCl [pH 8.1], 500 mmol/L NaCl), LiCl wash buffer (250 mmol/L LiCl, 1% NP-40, 1% de-

oxycholate, 1.0 mmol/L EDTA, 1.0 mmol/L Tris-HCl [pH 8.1]) and Tris-EDTA buffer. Immunoprecipitated chromatin fragments were eluted with elution buffer (1% sodium dodecyl sulfate, 100 mmol/L NaHCO3, 10 mmol/L dithiothreitol), and reverse cross-linked by incubating for 6 hours at 65°C in elution buffer containing 200 mmol/L NaCl. DNA fragments were purified and quantified by real-time detection PCR with primers for putative ISRE in the 2′5′OAS promoter region (forward, 5′-AAA TGC ATT TCC AGA GCA GAG TTC AGA G-3′, reverse, 5′-GGG TAT TTC TGA GAT CCA TCA TTG ACA GG-3′) or putative FBE in the Socs3 promoter region (forward, 5′-TGC TGC GAG TAG TGA CTA AAC ATT ACA AG -3′, reverse, 5′-AGC GGA GCA GGG AGT CCA AGT C -3′). Values were normalized by the measurement of input DNA.

pH77S.3/GLuc2A

pH77S.2 is a modification of pH77S[2] containing an additional mutation within the E2 protein (N476D in the polyprotein) that promotes infectious virus yields from RNA-transfected cells (Yi et al, unpublished data). To monitor replication, the GLuc sequence, fused at its C terminus to the foot-and-mouth disease virus 2A autoprotease, was inserted between p7 and NS2 of pH77S.2 (Supplementary Figure 4). To insert the GLuc-coding sequence between p7 and NS2 in pH77S.2, followed by the foot-and-mouth disease virus 2A protein-coding sequence, Mlu I, EcoR V, and Spe I restriction sites were created between the p7 and NS2 coding sequences by site-directed mutagenesis. DNA coding for GLuc was subcloned into the Mlu I and EcoR V sites of the modified plasmid after PCR amplification using the primers: 5′- ATA ATA TTA CGC GTA *TGG GAG TCA AAG TTC TGT TTG CC*-3′ (sequence corresponding to the N-terminal GLuc is italicized and that corresponding to Mlu I is underlined) and 5′-ATA AAT AGAT ATC *GTC ACC ACC GGC CCC CTT GAT CTT*-3′ (C terminal GLuc is italicized and EcoR V is underlined). A DNA fragment encoding the 17 amino acids of the foot-and-mouth disease virus 2A protein was generated by annealing the following complementary oligonucleotides: 5′- ATA TGA TAT CAA CTT TGA CCT TCT CAA GTT GGC CGG CGA CGT CGA GTC CAA CCC AGG GCC CAC TAG CAT AT-3′ and 5′-ATA TGC TAG TGG GCC CTG GGT TGG ACT CGA CGT CGC CGG CCA ACT TGA GAA GGT CAA AGT TGA TAT CAT AT-3′ (underlined sequences indicate EcoR V and Spe I sites). The annealed oligonucleotides were digested by both restriction enzymes and the product inserted into the corresponding sites of pH77S.2 containing GLuc to generate pH77S.2/GLuc2A. Q41R is a cell-culture adaptive mutation within the NS3 protease domain of pH77S. Because it is not essential for production of infectious virus (Yi et al, unpublished data), pH77S.2 and pH77S.2/GLuc2A constructs underwent this mutation by site-directed mutagenesis of a PCR fragment spanning the Afe I and BsrG I sites to replace Gln_{41} with wild-type Arg. The resulting plasmids (pH77S.2/R41Q and pH77S.2/GLuc2A/R41Q) were redesignated pH77S.3 and pH77S.3/GLuc2A, respectively.[3,4] GLuc has several advantages over other luciferase reporter enzymes in that it is smaller and allows more sensitive detection than either firefly or Renilla luciferase.[3,4] In addition, a signal sequence directs its secretion into cell-culture media, allowing real-time dynamic measurements of GLuc expression without the need for cell lysis. H77S.3/GLuc2A RNA produces infectious virus, although with lower efficiency than H77S.3 RNA (10-fold less).

References

1. Shimbo K, Kubo S, Harada Y, et al. Automated precolumn derivatization system for analyzing physiological amino acids by liquid chromatography/mass spectrometry. Biomed Chromatogr 2009; 24:683–691.
2. Yi M, Villanueva RA, Thomas DL, et al. Production of infectious genotype 1a hepatitis C virus (Hutchinson strain) in cultured human hepatoma cells. Proc Natl Acad Sci U S A 2006;103:2310–2315.
3. Shetty S, Kim S, Shimakami T, et al. Hepatitis C virus genomic RNA dimerization is mediated via a kissing complex intermediate. RNA 2010;16:913–925.
4. Shimakami T, Welsch C, Yamane D, et al. Protease inhibitor-resistant hepatitis C virus mutants with reduced fitness from impaired production of infectious virus. Gastroenterology 2011; 140:667–675.

Cancer Letters 307 (2011) 165–173

Contents lists available at ScienceDirect

Cancer Letters

journal homepage: www.elsevier.com/locate/canlet

Frequency of CD45RO$^+$ subset in CD4$^+$CD25^{high} regulatory T cells associated with progression of hepatocellular carcinoma

Yoshiko Takata [a], Yasunari Nakamoto [a], Akiko Nakada [b], Takeshi Terashima [a], Fumitaka Arihara [a], Masaaki Kitahara [a], Kaheita Kakinoki [a], Kuniaki Arai [a], Taro Yamashita [a], Yoshio Sakai [a], Tatsuya Yamashita [a], Eishiro Mizukoshi [a], Shuichi Kaneko [a,*]

[a] Disease Control and Homeostasis, Graduate School of Medicine, Kanazawa University, 13-1 Takara-machi, Kanazawa 920-8641, Japan
[b] Otsuka Pharmaceutical Co., Ltd., 2-16-4 Konan, Minato-ku, Tokyo 108-8242, Japan

ARTICLE INFO

Article history:
Received 31 December 2010
Received in revised form 11 March 2011
Accepted 30 March 2011

Keywords:
Regulatory T cell
Dendritic cell
Hepatocellular carcinoma
CD45RO
Intracellular cytokine

ABSTRACT

The purpose of this study was to assess the properties of CD4$^+$CD25$^{high/low/negative}$ T cell subsets and analyze their relation with dendritic cells (DCs) in patients with hepatocellular carcinoma (HCC). In HCC patients, the prevalence of CD45RO$^+$ cells in CD4$^+$CD25^{high} T cells was increased and associated with higher frequencies of plasmacytoid DCs. Larger proportions of this T cell subset were detected in the patients with larger tumor burdens. These results suggest that increased frequencies of the CD45RO$^+$ subset in CD4$^+$CD25^{high} Tregs in HCC patients may establish the immunosuppressive environment cooperatively with tolerogenic plasmacytoid DCs to promote disease progression of liver cancer.

1. Introduction

Hepatocellular carcinoma (HCC) occurs primarily in individuals with cirrhosis related to hepatitis C virus (HCV) or hepatitis B virus (HBV) infections, and alcohol abuse. HCC is the fifth most common cancer, with increasing incidence worldwide. It is characterized by high mortality, frequent postsurgical recurrence and extremely poor prognosis [1–3].

CD4$^+$CD25^{high} Foxp3$^+$ regulatory T cells (Tregs) have been shown to suppress immune responses by direct interaction with other immune cell types or through immune suppressive cytokines and appear crucial in maintaining immune homeostasis, mediating peripheral tolerance and preventing autoimmunity [4–6]. Increased frequencies of Tregs have been documented in the peripheral blood and in some cases the tumor microenvironment in patients with several different tumor types [3–12]. It has been reported that, in HCC patients, increased Tregs are correlated with CD8$^+$ T-cell impairment [11] and are related to poor prognosis [1].

Tregs are known to consist of heterogeneous subsets and to express various surface markers detectable by flow cytometry, including CD45RO, CTLA-4 (cytotoxic T lymphocyte associated antigen-4), GITR (glucocorticoid-induced TNF receptor-related protein), CD62L, HLA-DR, and CCR7 [8,13–15]. The role of these markers in suppressor functions mediated by human Tregs is currently under discussion [8]. It has been suggested that GITR is associated with T cell activation [16,17] and Treg subset expressing GITR are associated with disease activity in patients with Wegener's granulomatosis [17]. As for HCC, Ormandy et al. demonstrated that Tregs in HCC patients expressed high levels of HLA-DR and GITR [3]. However, there is a paucity of studies presenting the association of Treg subsets with disease progression.

In addition to Tregs, dendritic cells (DCs), a type of professional antigen-presenting cells (APCs), may be

* Corresponding author. Tel.: +81 76 265 2233; fax: +81 76 234 4250.
E-mail address: skaneko@m-kanazawa.jp (S. Kaneko).

0304-3835/$ - see front matter © 2011 Published by Elsevier Ireland Ltd.
doi:10.1016/j.canlet.2011.03.029

implicated in the regulation of immune responses. The role of human DCs in modulating Tregs is not clear [18]. It has been suggested that immature and mature myeloid DCs (mDCs) and plasmacytoid DCs (pDCs) may promote Treg cell differentiation, homeostasis and function [19]. It has been shown that lung cancer cells can convert mature DCs into TGF-β1 producing cells, which demonstrate an increased ability to generate Tregs [20]. Conversely, Tregs can induce the generation of semimature DCs by which they can down-regulate immune responses [21]. These data suggest that there may be a mutual interaction between Tregs and DCs for the maintenance of immunosuppression.

In the present study, we evaluated the frequency and properties of $CD4^+CD25^{high}$ $Foxp3^+$ T cells in HCC patients. Increased numbers of these cells produced more Th2 cytokine than $CD4^+CD25^{low/negative}$ cells. Furthermore, the proportion of $CD45RO^+$ subset was increased in HCC patients. We also analyzed how the subset is related to DC frequencies, and found that some subsets were relevant to disease progression.

2. Materials and methods

2.1. Patients and healthy controls

Sixty-two HCC patients attending Kanazawa University Hospital (Ishikawa, Japan) between September 2006 and July 2008 were enrolled in this study with their informed consent. HCC was radiologically diagnosed by computed tomography (CT), magnetic resonance imaging (MRI), and CT angiography. Blood samples were taken from these HCC patients, as well as from 41 healthy controls, 17 patients with chronic hepatitis (CH) B and C and 16 patients with liver cirrhosis (LC) without a tumor. None of the patients received anticancer nor antiviral therapy at time of blood sample. Patients characteristics and disease classification are shown in Table 1.

Table 1
Clinical characteristics of hepatocellular carcinoma, liver cirrhosis, chronic hepatitis patients and healthy control.

Hepatocellular carcinoma (n = 62)	
Age (yrs)	68.9 ± 9.5
Gender (M/F)	37/25
Etiology of liver disease	
HBV/HCV/HBV + HCV/NBNC	19/34/2/7
TNM stages I/II/III/IV-A/IV-B	18/12/20/6/6
Largest tumor (mm)	
Child-Pugh A/B/C	37.6 ± 34.4
AFP (ng/mL)	41/8/3
DCP (mAU/mL)	10–35,093 (52)
Liver cirrhosis (n = 16)	
Age (yrs)	10–32,818 (34)
Gender (M/F)	58.3 ± 10.3
Etiology of liver disease	11/5
HBV/HCV/NBNC	4/7/5
Chronic hepatitis (n = 17)	
Age (yrs)	58.9 ± 10.4
Gender (M/F)	8/9
Etiology of liver disease	
HBV/HCV/NBNC	0/17/0
Healthy controls (n = 41)	
Age (yrs)	46.1 ± 19.1
Gender (M/F)	16/25

Note: Results except for AFP and DCP are expressed as means ± SD. AFP and DCP values are expressed as range (median). The reference range of normal values for the laboratory values: AFP < 10 ng/mL, DCP < 40 mAU/mL. M, Male; F, Female; HBV, hepatitis B virus; HCV, hepatitis C virus; NBNC, non-B non-C; TNM, tumor-node-metastasis; AFP, alpha-fetoprotein; DCP, des-gamma-carboxy prothrombin.

2.2. Isolation of PBMC and $CD4^+$ T cells

Peripheral blood mononuclear cells (PBMC) were isolated from freshly obtained blood by Ficoll-Hypaque (Sigma–Aldrich, St. Louis, MO). Total cell numbers were counted in the presence of a trypan blue dye to evaluate viability and immediately used for experiments. $CD4^+$ T cells were isolated from fleshly isolated PBMC by negative magnetic selection using the $CD4^+$ T Cell Isolation Kit II (Miltenyi Biotec, Bergisch Gladbach, Germany) and QuadroMACS Separation Unit (Miltenyi Biotec) according to the manufacturer's instruction. Isolated $CD4^+$ T cells were purified by >90% as measured by flow cytometric analysis using a FACSCaliber flow cytometer (BD Biosciences, San Jose, CA).

2.3. Antibodies

The following anti-human monoclonal antibodies (mAb) were used for flow cytometry: anti-CD4-PerCP, anti-CD25-APC (BD Biosciences, San Jose, CA), anti-CD45RO-FITC (PROIMMUNE, Oxford, UK), anti-CTLA-4-PE, anti-CCR7-PE, anti-GITR (glucocorticoid-induced TNF receptor-related protein)-PE (R&D Systems, Minneapolis, MN), anti-CD62L-FITC, anti-HLA-DR-FITC, anti-CD45RA-PE (Exalpha Biologicals, Watertown, MA), IOTest Conjugated Antibodies – (CD14 + CD16)-FITC/CD85k(ILT3)-PE/CD123-PC5 Dendritic Cells " Plasmacytoid Subset " and IOTest Conjugated Antibodies – (CD14 + CD16)-FITC/CD85k(ILT3)-PE/CD33-PC5 Dendritic Cells "Myeloid Subset " (Beckman Coulter, Miami, FL). Before use, all mAbs were titrated using normal PBMC to establish optimal staining dilutions.

2.4. Surface and intracellular staining

To determine the frequency of $CD4^+CD25^{high}$ T cells and the surface marker profile, $CD4^+$ T cells (at least 2×10^5 cells/tube) were stained with mAbs in the above described panel for 30 min on ice. Apropriate isotype antibody controls were used for each sample. Cells were washed and examined by four-color flow cytometry.

For intracellular Foxp3 and cytokine staining, 2×10^5 $CD4^+$ T cells/well in a 96-plate were stimulated with Leucocyte Activation Cocktail containing PMA, ionomycin, and brefeldin A, and then cultured at 37 °C in a humidified CO_2 incubator for 4 h. The activated cells were first incubated with anti-CD4-PerCP for 15 min on ice, followed by fixation and permeabilization of the activated cells for 20 min at room temperature with BD Cytofix/Cytoperm Buffer (BD Biosciences, San Diego, CA). Samples were then stained with anti-CD25-APC, anti-Foxp3-FITC (eBioscience) and PE-labeled anti-cytokine (IL-4, IL-10) antibodies (BD

Biosciences) for 15 min at room temperature. Apropriate isotype controls were included for each sample.

2.5. Flow cytometric analysis

The samples were acquired on a FACSCalibur for four-color flow cytometry. Data analysis was performed using the CellQuest software (Becton Dickinson, CA, USA).

2.6. Statistical analysis

Data are indicated as means ± SD unless otherwise stated. The statistical significance of difference between the two groups was determined by applying the Mann–Whitney nonparametric U test. $P < 0.05$ was considered significant.

3. Results

3.1. Frequencies of $CD4^+CD25^{high}$ T cells

To evaluate the frequencies of $CD4^+CD25^{high}$ T cell subsets that contain Tregs, MACS-sorted $CD4^+$ T cell subsets obtained from the patients with CH, LC and HCC and healthy controls were analyzed by flow cytometry following the staining with anti-CD4 and anti-CD25 monoclonal antibodies (Fig. 1A and B). Although the frequencies of $CD4^+CD25^{high}$ T cells were not changed in patients with CH, they were increased in patients with LC compared to the controls ($P < 0.05$). As reported, it is remarkably elevated in patients with HCC ($P < 0.0001$). The results indicated that $CD4^+CD25^{high}$ T cell subset containing Tregs are increased in patients complicated with liver malignancies.

3.2. Intracellular Foxp3 and cytokine production of the $CD4^+CD25^{high}$ T cell subset in HCC patients

The transcription factor Foxp3 is considered to be a specific marker for Tregs [22–24]. Intracellular Foxp3 levels were detected by using the specific mAb after the cell membrane permeabilization procedures (Fig. 2A). The percent of $Foxp3^+$ cells in the $CD4^+CD25^{high}$ T cell subset in HCC patients was larger than that of $CD4^+CD25^{low/negative}$ subset, and it was also significantly larger than that of $CD4^+CD25^{high}$ T cells in healthy controls and CH patients (Fig. 2B). Thus, not only is the number of $CD4^+CD25^{high}$ T cells in HCC patients larger, but also the frequency of $Foxp3^+$ cells in HCC patients is higher than CH patient and healthy controls. This is consistent with previous reports of Tregs in patients with other malignancies.

Intracellular production of cytokines IL-4 and IL-10 of $CD4^+CD25^{high}$-$Foxp3^+$ T cell subset was quantitated following the stimulation with PMA/ionomycin using the specific mAbs by flow cytometry (Fig. 2C).

The levels of Th2 cytokines IL-4 and IL-10 were high in the $CD4^+CD25^{high}$ subsets. In addition, the levels of IL-4 and IL-10 were high in the $CD4^+CD25^{high}Foxp3^+$ T cell subset in HCC patient ($P < 0.005$) (Fig. 2D). These results suggest that the $CD4^+CD25^{high}Foxp3^+$ Treg subset in HCC patients may have a high potential to produce immunosuppressive cytokines.

3.3. Phenotypes of the $CD4^+CD25^{high}$ T cell subset in HCC patients

To determine the phenotypical properties of $CD4^+CD25^{high}$ T cell subset increased in patients with HCC, the expression levels of the seven reported surface molecules, CD45RA, CD45RO, CD62L, CCR7, CTLA-4, HLA-DR and GITR were quantitated by flow cytometry. Among the seven molecules, the proportions of $CD45RO^+$, $HLA\text{-}DR^+$ and $GITR^+$ cells were higher in the $CD4^+CD25^{high}$ T cell subset in all patient groups compared to the $CD4^+CD25^{low/negative}$ T cell subsets, except for $GITR^+$ cells in CH patients ($P < 0.05$) (Fig. 3A and B). The percentage of $CD45RO^+$ cells in HCC patients were elevated compared to the patients with advanced liver diseases and healthy controls ($P < 0.01$). These data demonstrate that the $CD4^+CD25^{high}$ T cell subset highly expresses the surface molecule CD45RO in HCC patients, which may reflect the memory properties of T cells.

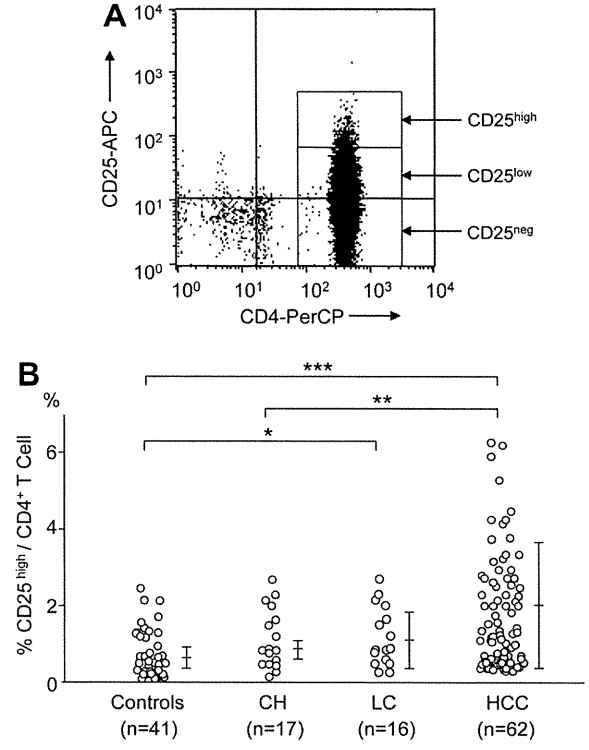

Fig. 1. Frequencies of $CD4^+CD25^{high}$ T cells in peripheral blood of HCC patients and controls. (A) Representative flow cytometric analysis of PBMCs (peripheral blood mononuclear cells) of an HCC patient. Freshly isolated PBMCs were labeled with anti-CD4 and anti-CD25 antibodies as described in the Materials and Methods. (B) Percentages of $CD4^+CD25^{high}$ T cells in the peripheral blood of HCC ($n = 62$), LC ($n = 16$), CH ($n = 17$) patient, and healthy controls ($n = 41$). Percentages for individual patient analyzed are shown. The percentages represent the proportions of $CD4^+CD25^{high}$ T cells in total $CD4^+$ cells. The prevalence of $CD4^+CD25^{high}$ T cells in HCC patients was significantly higher than in healthy controls or CH patients. CH, chronic hepatitis; HCC, hepatocellular carcinoma; LC, liver cirrhosis. *Indicates $P < 0.05$, **indicates $P < 0.01$ and ***indicates $P < 0.001$.

3.4. $CD4^+CD25^{high}$ T Cell subset and dendritic cells of HCC patients

Several reports have suggested that the $CD4^+CD25^{high}$ T cell subset may interact with dendritic cells. To evaluate the frequencies of DCs in PBMC of HCC patients, whole blood cells were analyzed by flow cytometry following the staining with IOTest Conjugated Antibodies – (CD14 + CD16)-FITC/CD85k(ILT3)-PE/CD123-PC5 Dendritic Cells "Plasmacytoid Subset" and IOTest Conjugated Antibodies – (CD14 + CD16)-FITC/CD85k(ILT3)-PE/CD33-PC5 Dendritic Cells "Myeloid Subset". HCC patients were divided into two groups according to the frequencies of $CD45RO^{positive}$ cells in $CD4^+CD25^{high}$ T cell subsets ($CD45RO^+$ vs. $CD45RO^{++}$). Patients with $CD45RO^{++}$ contained >83.8% positive cells in $CD4^+CD25^{high}$ T cells. The frequencies of $CD123^+$ plasmacytoid DCs were significantly higher in $CD45RO^{++}$, group ($P < 0.05$) (Fig. 5A and B), although those of $CD33^+$ myeloid DCs were not correlated with the subsets in $CD4^+CD25^{high}$ cells. These results showed that there are more tolerogenic plasmacytoid DCs in the PBMCs of HCC patients with higher frequencies of a memory subset of $CD4^+CD25^{high}$ T cells.

3.5. $CD4^+CD25^{high}$ T cell subset and tumor progression

To evaluate the association between $CD4^+CD25^{high}$ T cell phenotype and tumor progression, we compared the maximum tumor diameters, the number of tumors, tumor markers AFP (alpha-fetoprotein) and DCP (des-gamma-carboxyl prothrombin), TNM stages, Child-Pugh scores

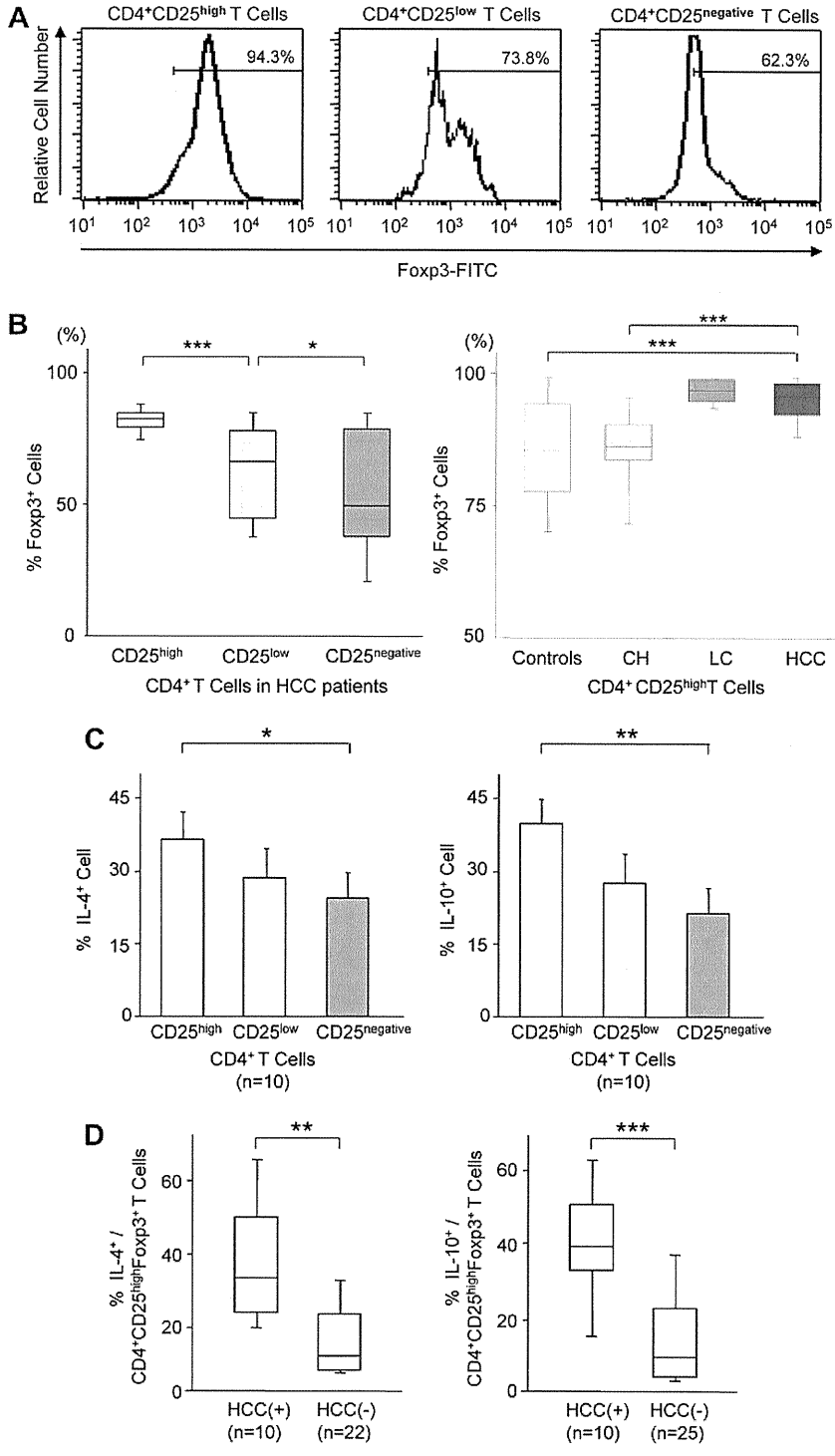

Fig. 2. Analysis of intracellular Foxp3 expression and cytokine production in $CD4^+$ $CD25^{high/low/negative}$ T cell subsets in HCC patients. (A) Representative expression of Foxp3 in $CD4^+$ T cells from an individual subject. Intracellular Foxp3 was stained following membrane permeabilization. Intracellular Foxp3 was detected by the specific mAb. (B) Statistical analysis in the left side panel shows that the percent of $Foxp3^+$ cells in the $CD4^+CD25^{high}$ T cell subset in HCC patients was significantly larger than that of $CD4^+CD25^{low/negative}$ T cell subsets, and in the right side panel shows that that of $CD4^+CD25^{high}$ T cell subset in HCC patients was significantly larger than that of $CD4^+CD25^{high}$ T cells in healthy controls and CH patients. (C) Statistical analysis shows that the levels of Th2 cytokines IL-4 and IL-10 were remarkably high in the $CD4^+CD25^{high}$ T cell subset. (D) Comparison of intracellular cytokine production in $CD4^+CD25^{high}$ T cell subsets between patients with and without HCC. Healthy controls, patients with chronic hepatitis and liver cirrhosis were included in the HCC (−) column. IL-4 and IL-10 levels were higher in the $CD4^+CD25^{high}$ T cell subset in HCC patients. *Indicates $P < 0.05$, **indicates $P < 0.01$ and ***indicates $P < 0.001$.

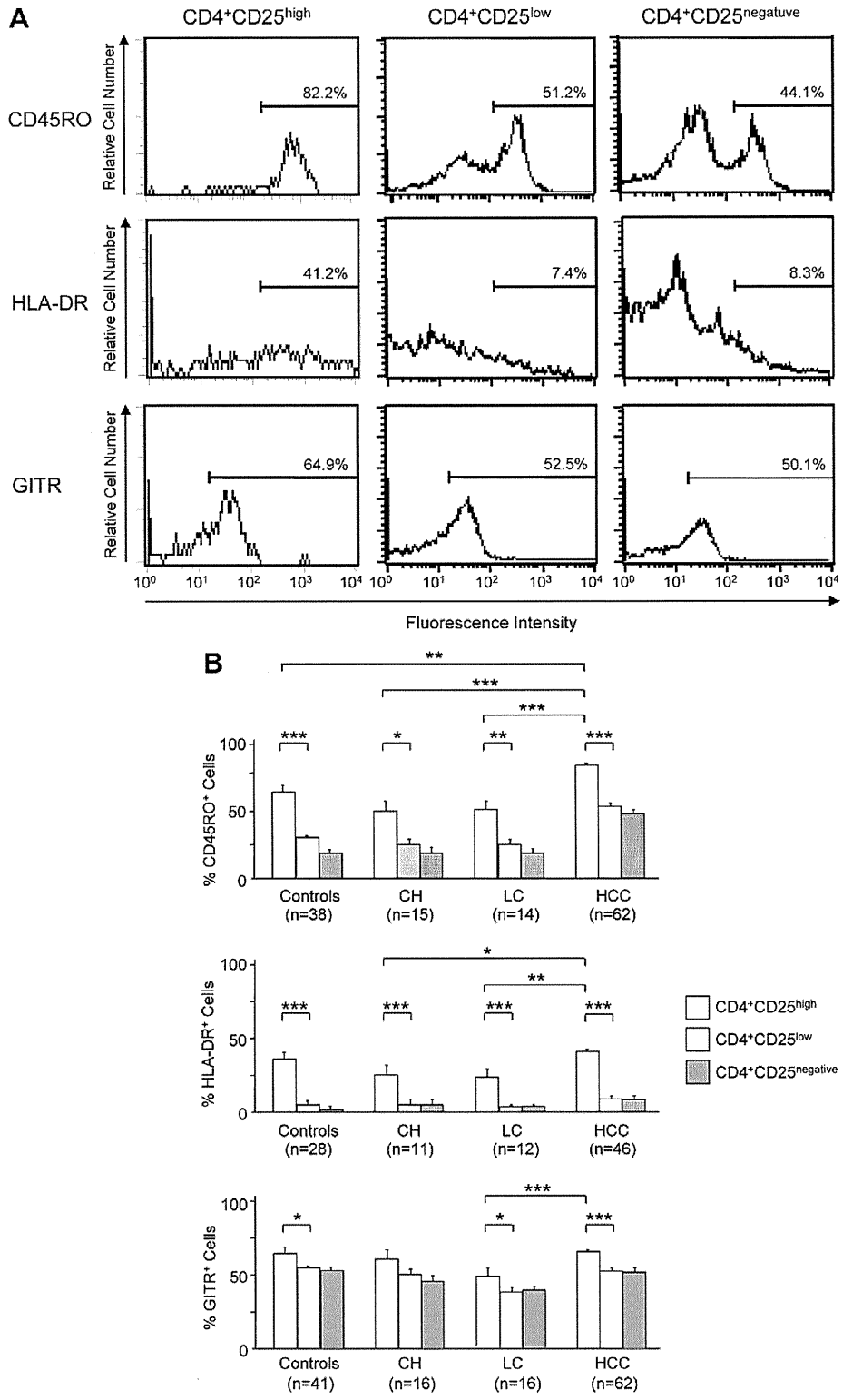

Fig. 3. Phenotypic analysis of $CD4^+CD25^{high/low/negative}$ T cell subsets in HCC patients. Fleshly isolated $CD4^+$ T cells (at least 2×10^5 cells/tube) from HCC patients were labeled with anti-CD4, anti-CD25, anti-CD45RA, anti-CD45RO, anti-CD62L, anti-CCR7, anti-CTLA-4, anti-HLA-DR and anti-GITR mAbs. (A) Representative CD45RO, HLA-DR, and GITR expression profiles in $CD4^+$ T cell subsets that differ in CD25 expression. (B) Statistical analysis shows that the proportions of $CD45RO^+$, $HLA\text{-}DR^+$ and $GITR^+$ were elevated in the $CD4^+CD25^{high}$ T cell subsets of all patient groups compared to the $CD4^+CD25^{low/negative}$ T cell subsets, except for $GITR^+$ cells in CH patients ($P < 0.05$). The percentage of $CD45RO^+$ cells in HCC patients was elevated compared to the patients with advanced liver diseases and healthy controls. *Indicates $P < 0.05$, **indicates $P < 0.01$ and ***indicates $P < 0.001$.

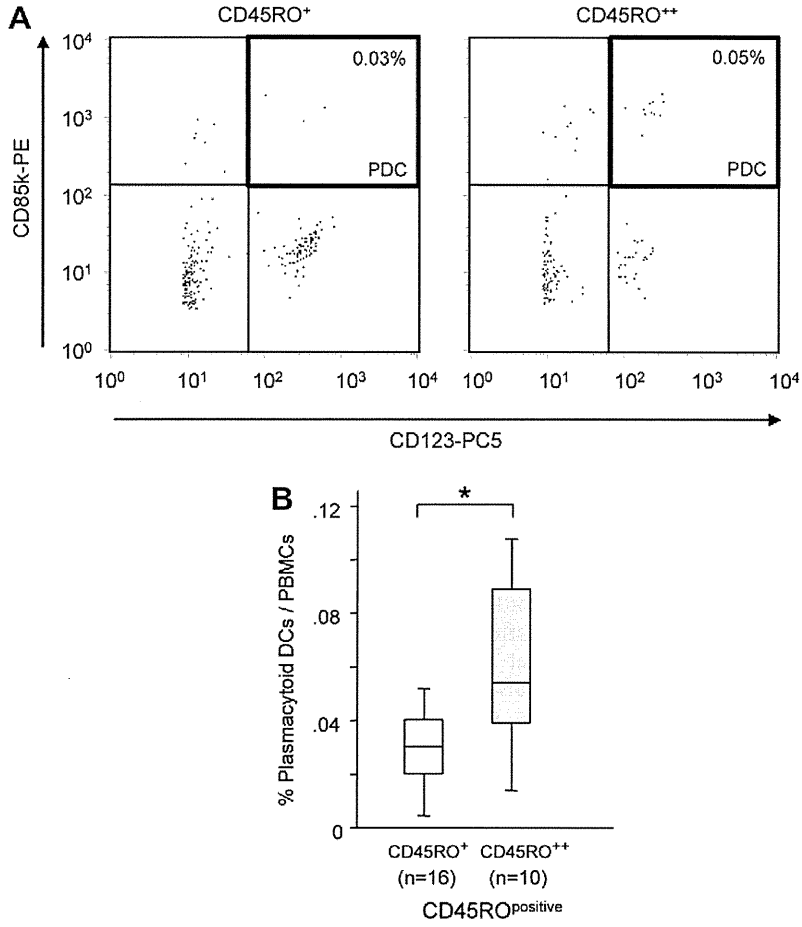

Fig. 4. Frequencies of plasmacytoid DCs in peripheral blood of HCC patients. Whole blood cells were analyzed by flow cytometry following staining with a combination of the mAbs. HCC patients were divided into two groups according to the frequencies of $CD45RO^{positivee}$ cells in $CD4^+CD25^{high}$ T cell subset ($CD45RO^+$ vs. $CD45RO^{++}$). Patients with $CD45RO^{++}$ contained > 83.8% positive cells in $CD4^+CD25^{high}$ T cells. (A) Representative dot plots of plasmacytoid DCs. Plasmacytoid DCs of $CD45RO^+$ group are shown in the left panel and $CD45RO^{++}$ group in the right panel. (B) Statistical analysis shows that the frequencies of plasmacytoid DCs were significantly higher in $CD45RO^{++}$ group. *Indicates $P < 0.05$.

and fibrosis stages between two groups as described above. The levels of serum AFP and DCP and the maximum tumor diameters in $CD45RO^{++}$ group were larger than those in $CD45RO^+$ group (Fig. 4). Others were not significantly different between two groups. These results imply that a subset of Tregs may contribute to the progression of liver tumors.

4. Discussion

$CD4^+CD25^{high}$ $Foxp3^+$ regulatory T cells have been shown to increase in patients with malignancies to suppress the immune responses. In this study, we provide evidence that patients with HCC have increased frequencies of $CD4^+CD25^{high}$ T cells in their peripheral blood compared to healthy controls and chronic hepatitis patients. A large proportion of $CD4^+CD25^{high}$ T cells expressed Foxp3 and produced Th2 cytokines. We also showed that $CD4^+CD25^{high}$ T cells expressed high levels of CD45RO, HLA-DR and GITR, and, interestingly, the T cell frequencies expressing these surface molecules were associated with plasmacytoid DC numbers and maximum tumor diameters in HCC patients.

There are several reports of elevated numbers of Treg cells in the peripheral blood and tumor tissues of patients with different types of cancer [3–12]. The study of Unitt et al. provided the first report of increased $CD4^+CD25^+$ T cell frequency within tumor tissue compared to non-tumor tissue in HCC patients [13]. Ormandy et al. showed that the frequency of $CD4^+CD25^{high}$ T cells in peripheral blood of patients with HCC was significantly higher ($3.92 \pm 3.3\%$) than in healthy donors ($1.17 \pm 0.87\%$) and liver cirrhosis patients ($0.78 \pm 0.43\%$) [3]. Our data revealed that a minimal increase in $CD4^+CD25^{high}$ T cells was detected in LC patients and more pronounced changes were found in HCC patients.

We showed that higher percentages of $CD4^+CD25^{high}$ T cells produced Th2 cytokines IL-4 and IL-10 in HCC patients. Tregs were recently observed to produce IL-10 [25–27], which can be a major mediator of immune suppression [28–30]. Voo et al. reported that Tregs in the peripheral blood of healthy donors secreted IL-10 but not IL-2, IFN-γ, or IL-4 [31]. Schmitz-Winnenthal et al. demon-

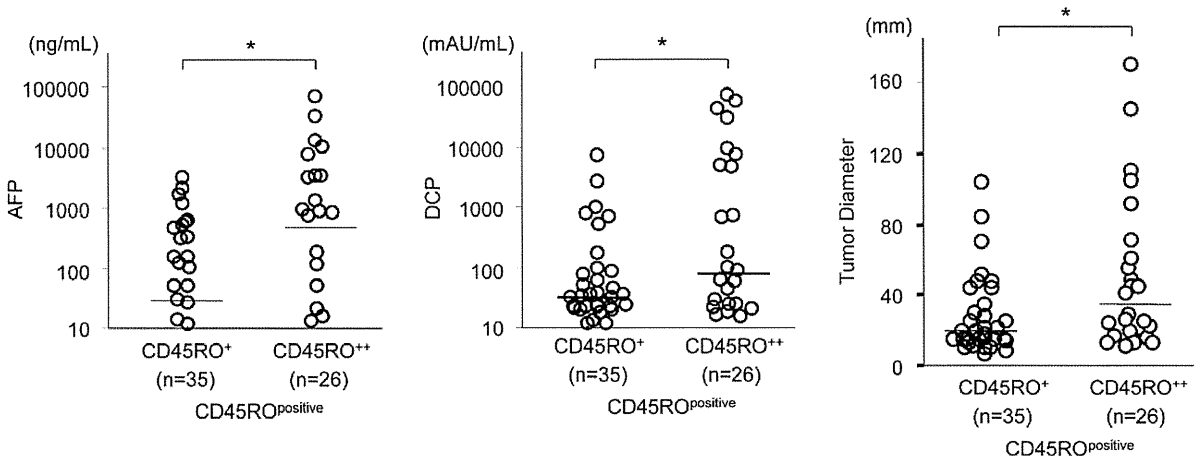

Fig. 5. Prevalence of $CD4^+CD25^{high/low/negative}$ T cell subsets and tumor progression. The levels of AFP and DCP and the maximum tumor diameters in $CD45RO^{++}$ group were larger than those in $CD45RO^+$ groups. AFP, alpha-fetoprotein; DCP, des-gamma-carboxyl prothrombin. *Indicates $P < 0.05$.

strated the presence of Treg secreting IL-10 but not IL-4 or IFN-γ upon antigen recognition in chronic pancreatitis patients [32]. The present data demonstrated that larger numbers of Tregs produced not only IL-10 but also IL-4 in HCC patients, which may contribute to the strong immunosuppressive properties of the T cells in liver malignancies.

It appears that Tregs consists of heterogenous populations within $CD4^+$ T cells, and that a subset of $CD4^+CD25^{high}$ T cells could be subdivided into different functional subsets based on the expression of various surface molecules [6]. The proportions of Tregs expressing these molecules are reported to be different in the various forms of cancer. The prevalence of $CD45RO^+$ and $GITR^+$ Treg cells is higher in $CD4^+CD25^{high}$ T cells than in $CD4^+CD25^{low/negative}$ T cells in renal cell carcinoma [4]. In head and neck squamous cell carcinoma, however, $CD4^+CD25^{high}$ T cells express CTLA-4, Foxp3, and CD62L but little GITR, and $CD25^{low/negative}$ T cells express intermediate to high levels of GITR and HLA-DR [8]. Our study showed that Tregs in HCC patients expressed significantly higher levels of CD45RO, HLA-DR and GITR compared to $CD4^+CD25^{low/negative}$ cells, suggesting that the activated populations of Tregs may contribute to the establishment of immunosuppressive microenvironments.

Little is known about the molecular and cellular mechanisms responsible for the increase and maintenance of elevated numbers of Treg cells in cancer. DCs have pivotal roles in the induction of tolerogenic/regulatory T cells [20,33]. In peripheral blood, there are two distinct populations of DCs which can be distinguished based on phenotypical and morphological characteristics; myeloid DCs (mDCs) and plasmacytoid DCs (pDCs) [18,34]. Our data demonstrated that higher frequencies of $CD45RO^+CD4^+CD25^{high}$ T cells were associated with higher frequencies of pDCs in the peripheral blood of HCC patients. When the tumor antigens are assumed by pDCs through Toll-like receptor 9 (TLR9) via receptor-mediated endocytosis, secretions of pro-inflammatory cytokines, such as type I interferons (IFNs), would be caused. On the contrary, pDC may regulate anti-tumor immunity and support immune evasion and tumor escape. They exhibit reduced IFN-α production upon TLR9 stimulation and can induce IL-10 producing $CD4^+$ and $CD8^+$ Treg [35,36]. This suggests that anti-tumor immune responses can be regulated through both modulation of pDC function by the tumor and by limiting anti-tumor cytolytic activity through induction of $CD8^+$ Treg.

Concerning the association of Tregs and prognosis, it has been reported that an increased number of circulating Tregs predicts poor survival of patients with renal cell carcinoma [4], gastric and esophageal cancers [7], myelodysplastic syndrome [37] and HCC [11]. In addition, tumor-infiltrating Tregs were associated with reduced survival in ovarian cancer [12] and HCC patients [1]. In addition, we found that $CD45RO^+CD4^+CD25^{high}$ T cell subset was associated with larger tumor burdens, implying that a subset of Tregs may contribute to the promotion of tumor cell growth in the liver. However, it is also well possible that this just reflects stronger activation caused by a larger amount of antigen.

We performed the functional evaluation of Tregs derived from HCC patients by incubating with responder $CD4^+CD25^-$ T cells (Tresp). We observed that $CD45RO^+$ $CD4^+CD25^{high}$ T cells of HCC patients did not suppress the proliferation of responder T cells when co-cultured at Treg/Tresp ratios of 1:2 and 1:8 (data not shown). In contrast, Hoffmann et al. confirmed that the $CD45RA^+$ $CD4^+CD25^{high}$ T cells of healthy volunteers give rise to a homogeneous and highly suppressive Treg cell population, whereas $CD45RA\text{-}CD4^+CD25^{high}$ T cells generate cell lines with mixed phenotype and function [38]. Although the reasons of these conflicting data were not clarified in the current study, cell viability, apoptosis susceptibility, involvement of Th1 cytokines, and interaction to helper T cell subsets of Tregs obtained from HCC patients need to be evaluated in the future experiments.

This study may be helpful for a better characterization of Treg subsets in the peripheral circulation of patients with HCC, which may establish the immunosuppressive environment to promote tumor progression. Furthermore, to gain insights into changes in the Treg subsets

during the therapeutic option may lead to more effective immunotherapies against cancer and may improve prognosis.

Conflict of interest

None declared.

Acknowledgements

We thank Ms. Mariko Katsuda for technical assistance. We also thank the patients for participating in this study.

References

[1] J. Zhou, T. Ding, W. Pan, L.Y. Zhu, L. Li, L. Zheng, Increased intratumoral regulatory T cells are related to intratumoral macrophages and poor prognosis in hepatocellular carcinoma patients, Int. J. Cancer 125 (2009) 1640–1648.
[2] Y. Nakamoto, E. Mizukoshi, H. Tsuji, Y. Sakai, M. Kitahara, K. Arai, T. Yamashita, K. Yokoyama, N. Mukaida, K. Matsushima, O. Matsui, S. Kaneko, Combined therapy of transcatheter hepatic arterial embolization with intratumoral dendritic cell infusion for hepatocellular carcinoma: clinical safety, Clin. Exp. Immunol. 147 (2007) 296–305.
[3] L.A. Ormandy, T. Hillemann, H. Wedemeyer, M.P. Manns, T.F. Greten, F. Korangy, Increased populations of regulatory T cells in peripheral blood of patients with hepatocellular carcinoma, Cancer Res. 65 (2005) 2457–2464.
[4] R.W. Griffiths, E. Elkord, D.E. Gilham, V. Ramani, N. Clarke, P.L. Stern, R.E. Hawkins, Frequency of regulatory T cells in renal cell carcinoma patients and investigation of correlation with survival, Cancer Immunol. Immunother. 56 (2007) 1743–1753.
[5] J. Visser, H.W. Nijman, B.N. Hoogenboom, P. Jager, D. van Baarle, E. Schuuring, W. Abdulahad, F. Miedema, A.G. van der Zee, T. Daemen, Frequencies and role of regulatory T cells in patients with (pre)malignant cervical neoplasia, Clin. Exp. Immunol. 150 (2007) 199–209.
[6] C. Schaefer, G.G. Kim, A. Albers, K. Hoermann, E.N. Myers, T.L. Whiteside, Characteristics of CD4+CD25+ regulatory T cells in the peripheral circulation of patients with head and neck cancer, Br. J. Cancer 92 (2005) 913–920.
[7] K. Kono, H. Kawaida, A. Takahashi, H. Sugai, K. Mimura, N. Miyagawa, H. Omata, H. Fujii, CD4(+)CD25 high regulatory T cells increase with tumor stage in patients with gastric and esophageal cancers, Cancer Immunol. Immunother. 55 (2006) 1064–1071.
[8] L. Strauss, C. Bergmann, W. Gooding, J.T. Johnson, T.L. Whiteside, The frequency and suppressor function of CD4+CD25highFoxp3+ T cells in the circulation of patients with squamous cell carcinoma of the head and neck, Clin. Cancer Res. 13 (2007) 6301–6311.
[9] A.M. Wolf, D. Wolf, M. Steurer, G. Gastl, E. Gunsilius, B. Grubeck-Loebenstein, Increase of regulatory T cells in the peripheral blood of cancer patients, Clin. Cancer Res. 9 (2003) 606–612.
[10] F. Ichihara, K. Kono, A. Takahashi, H. Kawaida, H. Sugai, H. Fujii, Increased populations of regulatory T cells in peripheral blood and tumor-infiltrating lymphocytes in patients with gastric and esophageal cancers, Clin. Cancer Res. 9 (2003) 4404–4408.
[11] J. Fu, D. Xu, Z. Liu, M. Shi, P. Zhao, B. Fu, Z. Zhang, H. Yang, H. Zhang, C. Zhou, J. Yao, L. Jin, H. Wang, Y. Yang, Y.X. Fu, F.S. Wang, Increased regulatory T cells correlate with CD8 T-cell impairment and poor survival in hepatocellular carcinoma patients, Gastroenterology 132 (2007) 2328–2339.
[12] T.J. Curiel, G. Coukos, L. Zou, X. Alvarez, P. Cheng, P. Mottram, M. Evdemon-Hogan, J.R. Conejo-Garcia, L. Zhang, M. Burow, Y. Zhu, S. Wei, I. Kryczek, B. Daniel, A. Gordon, L. Myers, A. Lackner, M.L. Disis, K.L. Knutson, L. Chen, W. Zou, Specific recruitment of regulatory T cells in ovarian carcinoma fosters immune privilege and predicts reduced survival, Nat. Med. 10 (2004) 942–949.
[13] E. Unitt, S.M. Rushbrook, A. Marshall, S. Davies, P. Gibbs, L.S. Morris, N. Coleman, G.J. Alexander, Compromised lymphocytes infiltrate hepatocellular carcinoma: the role of T-regulatory cells, Hepatology 41 (2005) 722–730.
[14] E. Biagi, I. Di Biaso, V. Leoni, G. Gaipa, V. Rossi, C. Bugarin, G. Renoldi, M. Parma, A. Balduzzi, P. Perseghin, A. Biondi, Extracorporeal photochemotherapy is accompanied by increasing levels of circulating CD4+CD25+GITR+Foxp3+CD62L+ functional regulatory T-cells in patients with graft-versus-host disease, Transplantation 84 (2007) 31–39.
[15] J.N. Stoop, R.G. van der Molen, C.C. Baan, L.J. van der Laan, E.J. Kuipers, J.G. Kusters, H.L. Janssen, Regulatory T cells contribute to the impaired immune response in patients with chronic hepatitis B virus infection, Hepatology 41 (2005) 771–778.
[16] R.W. van Olffen, N. Koning, K.P. van Gisbergen, F.M. Wensveen, R.M. Hoek, L. Boon, J. Hamann, R.A. van Lier, M.A. Nolte, GITR triggering induces expansion of both effector and regulatory CD4+ T cells in vivo, J. Immunol. 182 (2009) 7490–7500.
[17] B. Wilde, S. Dolff, X. Cai, C. Specker, J. Becker, M. Totsch, U. Costabel, J. Durig, A. Kribben, J.W. Tervaert, K.W. Schmid, O. Witzke, CD4+CD25+ T-cell populations expressing CD134 and GITR are associated with disease activity in patients with Wegener's granulomatosis, Nephrol. Dial. Transplant 24 (2009) 161–171.
[18] J.S. Ahn, D.K. Krishnadas, B. Agrawal, Dendritic cells partially abrogate the regulatory activity of CD4+CD25+ T cells present in the human peripheral blood, Int. Immunol. 19 (2007) 227–237.
[19] Q. Tang, J.A. Bluestone, Plasmacytoid DCs and T(reg) cells: casual acquaintance or monogamous relationship?, Nat Immunol. 7 (2006) 551–553.
[20] I.E. Dumitriu, D.R. Dunbar, S.E. Howie, T. Sethi, C.D. Gregory, Human dendritic cells produce TGF-beta 1 under the influence of lung carcinoma cells and prime the differentiation of CD4+CD25+Foxp3+ regulatory T cells, J. Immunol. 182 (2009) 2795–2807.
[21] J. Bayry, F. Triebel, S.V. Kaveri, D.F. Tough, Human dendritic cells acquire a semimature phenotype and lymph node homing potential through interaction with CD4+CD25+ regulatory T cells, J. Immunol. 178 (2007) 4184–4193.
[22] S. Hori, T. Nomura, S. Sakaguchi, Control of regulatory T cell development by the transcription factor Foxp3, Science 299 (2003) 1057–1061.
[23] H. Yagi, T. Nomura, K. Nakamura, S. Yamazaki, T. Kitawaki, S. Hori, M. Maeda, M. Onodera, T. Uchiyama, S. Fujii, S. Sakaguchi, Crucial role of FOXP3 in the development and function of human CD25+CD4+ regulatory T cells, Int. Immunol. 16 (2004) 1643–1656.
[24] J.D. Fontenot, M.A. Gavin, A.Y. Rudensky, Foxp3 programs the development and function of CD4+CD25+ regulatory T cells, Nat. Immunol. 4 (2003) 330–336.
[25] C.L. Maynard, L.E. Harrington, K.M. Janowski, J.R. Oliver, C.L. Zindl, A.Y. Rudensky, C.T. Weaver, Regulatory T cells expressing interleukin 10 develop from Foxp3+ and Foxp3- precursor cells in the absence of interleukin 10, Nat. Immunol. 8 (2007) 931–941.
[26] C.M. Freeman, B.C. Chiu, V.R. Stolberg, J. Hu, K. Zeibecoglou, N.W. Lukacs, S.A. Lira, S.L. Kunkel, S.W. Chensue, CCR8 is expressed by antigen-elicited, IL-10-producing CD4+CD25+ T cells, which regulate Th2-mediated granuloma formation in mice, J. Immunol. 174 (2005) 1962–1970.
[27] H.H. Uhlig, J. Coombes, C. Mottet, A. Izcue, C. Thompson, A. Fanger, A. Tannapfel, J.D. Fontenot, F. Ramsdell, F. Powrie, Characterization of Foxp3+CD4+CD25+ and IL-10-secreting CD4+CD25+ T cells during cure of colitis, J. Immunol. 177 (2006) 5852–5860.
[28] A. Wakkach, S. Augier, J.P. Breittmayer, C. Blin-Wakkach, G.F. Carle, Characterization of IL-10-secreting T cells derived from regulatory CD4+CD25+ cells by the TIRC7 surface marker, J. Immunol. 180 (2008) 6054–6063.
[29] M. Torisu, H. Murakami, F. Akbar, H. Matsui, Y. Hiasa, B. Matsuura, M. Onji, Protective role of interleukin-10-producing regulatory dendritic cells against murine autoimmune gastritis, J. Gastroenterol. 43 (2008) 100–107.
[30] M. Bettini, D.A. Vignali, Regulatory T cells and inhibitory cytokines in autoimmunity, Curr. Opin. Immunol. 21 (2009) 612–618.
[31] K.S. Voo, Y.H. Wang, F.R. Santori, C. Boggiano, K. Arima, L. Bover, S. Hanabuchi, J. Khalili, E. Marinova, B. Zheng, D.R. Littman, Y.J. Liu, Identification of IL-17-producing FOXP3+ regulatory T cells in humans, Proc. Natl. Acad. Sci. USA 106 (2009) 4793–4798.
[32] H. Schmitz-Winnenthal, D.H. Pietsch, S. Schimmack, A. Bonertz, F. Udonta, Y. Ge, L. Galindo, S. Specht, C. Volk, K. Zgraggen, M. Koch, M.W. Buchler, J. Weitz, P. Beckhove, Chronic pancreatitis is associated with disease-specific regulatory T-cell responses, Gastroenterology 138 (2010) 1178–1188.
[33] B. Eksteen, J.M. Neuberger, Mechanisms of disease: the evolving understanding of liver allograft rejection, Nat. Clin. Pract. Gastroenterol. Hepatol. 5 (2008) 209–219.
[34] Shiina, K. Kobayashi, T. Kobayashi, Y. Kondo, Y. Ueno, T. Shimosegawa, Dynamics of immature subsets of dendritic cells during antiviral therapy in HLA-A24-positive chronic hepatitis C patients, J. Gastroenterol. 41 (2006) 758–764.

[35] J. Charles, J. Di Domizio, D. Salameire, N. Bendriss-Vermare, C. Aspord, R. Muhammad, C. Lefebvre, J. Plumas, M.T. Leccia, L. Chaperot, Characterization of circulating dendritic cells in melanoma: role of CCR6 in plasmacytoid dendritic cell recruitment to the tumor, J. Invest. Dermatol. 130 (2010) 646–656.
[36] S. Wei, I. Kryczek, L. Zou, B. Daniel, P. Cheng, P. Mottram, T. Curiel, A. Lang, W. Zou, Plasmacytoid dendritic cells induce CD8+ regulatory T cells in human ovarian carcinoma, Cancer Res. 65 (2005) 5020–5026.
[37] S.Y. Kordasti, W. Ingram, J. Hayden, D. Darling, L. Barber, B. Afzali, G. Lombardi, M.W. Wlodarski, J.P. Maciejewski, F. Farzaneh, G.J. Mufti, CD4+CD25high Foxp3+ regulatory T cells in myelodysplastic syndrome (MDS), Blood 110 (2007) 847–850.
[38] P. Hoffmann, R. Eder, T.J. Boeld, K. Doser, B. Piseshka, R. Andreesen, M. Edinger, Only the CD45RA+ subpopulation of CD4+CD25high T cells gives rise to homogeneous regulatory T-cell lines upon in vitro expansion, Blood 108 (2006) 4260–4267.

OPEN ACCESS Freely available online

PLoS one

Sequence Heterogeneity in NS5A of Hepatitis C Virus Genotypes 2a and 2b and Clinical Outcome of Pegylated-Interferon/Ribavirin Therapy

Ahmed El-Shamy[1,2], Ikuo Shoji[1], Soo-Ryang Kim[3], Yoshihiro Ide[1], Susumu Imoto[3], Lin Deng[1], Seitetsu Yoon[4], Takashi Fujisawa[5], Satoshi Tani[6], Yoshihiko Yano[7], Yasushi Seo[7], Takeshi Azuma[7], Hak Hotta[1]*

1 Division of Microbiology, Center for Infectious Diseases, Kobe University Graduate School of Medicine, Kobe, Japan, **2** Department of Virology, Suez Canal University Faculty of Veterinary Medicine, Ismalia, Egypt, **3** Division of Gastroenterology, Kobe Asahi Hospital, Kobe, Japan, **4** Department of Gastroenterology, Hyogo Prefectural Kakogawa Medical Center, Kakogawa, Hyogo, Japan, **5** Department of Internal Medicine, Nippon Steel Hirohata Hospital, Himeji, Hyogo, Japan, **6** Department of Internal Medicine, Konan Hospital, Kobe, Japan, **7** Division of Gastroenterology, Department of Internal Medicine, Kobe University Graduate School of Medicine, Kobe, Japan

Abstract

Pegylated-interferon plus ribavirin (PEG-IFN/RBV) therapy is a current standard treatment for chronic hepatitis C. We previously reported that the viral sequence heterogeneity of part of NS5A, referred to as the IFN/RBV resistance-determining region (IRRDR), and a mutation at position 70 of the core protein of hepatitis C virus genotype 1b (HCV-1b) are significantly correlated with the outcome of PEG-IFN/RBV treatment. Here, we aimed to investigate the impact of viral genetic variations within the NS5A and core regions of other genotypes, HCV-2a and HCV-2b, on PEG-IFN/RBV treatment outcome. Pretreatment sequences of NS5A and core regions were analyzed in 112 patients infected with HCV-2a or HCV-2b, who were treated with PEG-IFN/RBV for 24 weeks and followed up for another 24 weeks. The results demonstrated that HCV-2a isolates with 4 or more mutations in IRRDR (IRRDR[2a]≥4) was significantly associated with rapid virological response at week 4 (RVR) and sustained virological response (SVR). Also, another region of NS5A that corresponds to part of the IFN sensitivity-determining region (ISDR) plus its carboxy-flanking region, which we referred to as ISDR/+C[2a], was significantly associated with SVR in patients infected with HCV-2a. Multivariate analysis revealed that IRRDR[2a]≥4 was the only independent predictive factor for SVR. As for HCV-2b infection, an N-terminal half of IRRDR having two or more mutations (IRRDR[2b]/N≥2) was significantly associated with RVR, but not with SVR. No significant correlation was observed between core protein polymorphism and PEG-IFN/RBV treatment outcome in HCV-2a or HCV-2b infection. ***Conclusion:*** The present results suggest that sequence heterogeneity of NS5A of HCV-2a (IRRDR[2a]≥4 and ISDR/+C[2a]), and that of HCV-2b (IRRDR[2b]/N≥2) to a lesser extent, is involved in determining the viral sensitivity to PEG-IFN/RBV therapy.

Citation: El-Shamy A, Shoji I, Kim S-R, Ide Y, Imoto S, et al. (2012) Sequence Heterogeneity in NS5A of Hepatitis C Virus Genotypes 2a and 2b and Clinical Outcome of Pegylated-Interferon/Ribavirin Therapy. PLoS ONE 7(2): e30513. doi:10.1371/journal.pone.0030513

Editor: John E. Tavis, Saint Louis University, United States of America

Received August 1, 2011; **Accepted** December 16, 2011; **Published** February 2, 2012

Funding: This study was supported in part by Health and Labour Sciences Research Grants from the Ministry of Health, Labour and Welfare, Japan, a J-GRID grant from the Ministry of Education, Culture, Sports, Science and Technology, Japan, and a SATREPS Grant from Japan Science and Technology Agency and Japan International Cooperation Agency. This study was also carried out as part of the Global Center of Excellence program of Kobe University Graduate School of Medicine. The funders had no role in study design, data collection and analysis, decision to publish, or preparation of the manuscript.

Competing Interests: The authors have declared that no competing interests exist.

* E-mail: hotta@kobe-u.ac.jp

Introduction

Hepatitis C virus (HCV) is a major cause of chronic liver disease, such as chronic hepatitis, liver cirrhosis and hepatocellular carcinoma, with180 million people being currently infected with HCV worldwide. It is estimated that 70% of acute infections become persistent [1]. As a consequence of the long-term persistence of HCV infection, the number of patients with hepatocellular carcinoma is expected to increase further over the next 20 years. More than two decades have passed since the discovery of HCV, and yet therapeutic options remain limited. Standard regimens for treatment of chronic hepatitis C include pegylated interferon alpha (PEG-IFN) and ribavirin (RBV) [2]. In addition, two protease inhibitors (telaprevir and boceprevir) were approved in May 2011 by the U. S. Food and Drug Administration (FDA) for clinical use in combination with PEG-IFN/RBV to treat chronic hepatitis C patients with HCV genotype 1 [3,4].

In Japan, about 70% of HCV-infected patients are infected with HCV genotype 1b (HCV-1b) and most of the remaining patients are infected with HCV-2a (25%) or HCV-2b (5%) [5]. When treated with PEG-IFN/RBV, the sustained virological response (SVR) rate is ca. 50% in HCV-1b infection, and ca. 80% in HCV-2a and -2b infections [2,6]. The mechanism(s) underlying the different responses among patients with different HCV genotypes and subtypes is still unclear. However, this suggests that viral genetic heterogeneity could affect, at least to some extent, the sensitivity to IFN-based therapy. In this context, sequence heterogeneity of the viral NS5A protein has been widely discussed for its correlation with IFN responsiveness. Sequence variations within a region in NS5A of HCV-1b defined as the IFN sensitivity-determining region (ISDR) is correlated with IFN responsiveness [7]. In HCV-2a infection, the influence of sequence heterogeneity in and around a region corresponding to ISDR on the IFN responsiveness was also suggested [8–10]. Recently, we identified a

new region near the C-terminus of NS5A of HCV-1b, which we refer to as the IFN/RBV resistance-determining region (IRRDR) [11,12]. The degree of sequence variation within IRRDR was significantly correlated with the clinical outcome of PEG-IFN/RBV combination therapy. The significance of IRRDR of other HCV genotypes, however, has not been investigated yet.

In addition to the NS5A sequence variation, HCV core protein polymorphism was also proposed as a pretreatment predictor of poor virological response in HCV-1b-infected patients treated with PEG-IFN/RBV therapy [13]. It is not clear at this stage whether core protein polymorphism could be used to predict the treatment outcome in HCV-2a and -2b infections. In the present study, we investigated the impact of viral genetic heterogeneity in the NS5A and core regions of HCV-2a and -2b on PEG-IFN/RBV treatment outcome. To the best of our knowledge, this is the first report describing the possible correlation between PEG-IFN/RBV responsiveness and NS5A-IRRDR heterogeneity of HCV-2a and -2b.

Materials and Methods

Ethics statement

The study protocol, which conforms to the provisions of the Declaration of Helsinki, was approved beforehand by the Ethic Committees in Kobe Asahi Hospital and Kobe University, and written informed consent was obtained from each patient prior to the treatment.

Patients

A total of 112 patients seen at Kobe Asahi Hospital and Kobe University Hospital, Kobe, Japan, who were chronically infected with HCV-2a (61 patients) or HCV-2b (51 patients), were enrolled in the study. HCV subtype was determined according to the method of Okamoto et al. [14]. The patients were treated with PEG-IFN α-2b (Pegintron®; Schering-Plough, Kenilworth, NJ) (1.5 μg per kilogram body weight, once weekly, subcutaneously) and RBV (Rebetol®; Schering-Plough) (600~800 mg daily, per os), for 24 weeks according to a standard treatment protocol for Japanese patients established by a hepatitis study group of the Ministry of Health, Labour and Welfare, Japan. All patients received >80% of scheduled dosage of PEG-IFN and RBV. Serum samples were collected from the patients at intervals of 4 weeks before, during and after the treatment, and tested for HCV RNA and core antigen titers as reported previously [15].

Sequence analysis of the NS5A and core regions

HCV RNA was extracted from 140 μl of serum using a commercially available kit (QIAmp viral RNA kit; QIAGEN, Tokyo, Japan). The extracted RNA was reverse transcribed and amplified for NS5A and core regions using Super script III one step RT-PCR platinum Taq HiFi (Invitrogen, Tokyo, Japan). The resultant RT-PCR product was subjected to a second-round PCR by using Platinum Taq DNA polymerase high fidelity III (Invitrogen). Primers used for amplification of full-length NS5A of the HCV-2a and -2b genomes and those of the core region of HCV-2a were reported previously [16,17]. Primers for amplification of the core region of HCV-2b are as follows: C-2b/1 (5′-AGCCATAGTGGTCTGCGGAACC-3′; sense, nucleotides [nt] 136 to 157) and C-2b/4 (5′-GGAACARTTGCACTCTTGG-GTG-3′; antisense, nt 1241 to 1262) for one step RT-PCR; C-2b/2 (5′-CCACTCTATGTCCGGTCATTTGG-3′; sense, nt 208 to 230) and C-2b/3 (5′-GAGCTGCCAGGTGATGCTG-3′; antisense, nt 971 to 989) for the second round PCR. RT was performed at 45°C for 30 min and terminated at 94°C for 2 min, followed by the first-round PCR over 35 cycles, with each cycle consisting of denaturation at 94°C for 30 sec, annealing at 55°C for 30 sec and extension at 68°C for 90 sec. The second-round PCR was performed under the same condition. The sequences of the amplified fragments were determined by direct sequencing without subcloning. The amino acid (aa) sequences were deduced and aligned using GENETYX Win software version 7.0 (GENETYX Corp., Tokyo, Japan). The numbering of aa residues for HCV-2a and -2b isolates is according to the polyprotein of HCV-J6 [18] and -J8 [19], respectively.

Statistical analysis

Numerical data were analyzed by *S*tudent's *t* test while categorical data by Fisher's exact probability test [8]. To evaluate the optimal threshold of the number of aa mutations in ISDR and IRRDR for prediction of treatment outcomes, the receiver operating characteristic curve was constructed. Univariate and multivariate logistic regression analyses were performed to identify independent predictors for treatment outcomes. All statistical analyses were performed using the SPSS version 16 software (SPSS Inc., Chicago, IL). Unless otherwise stated, a P value of <0.05 was considered statistically significant.

Nucleotide sequence accession numbers

The sequence data reported in this paper have been deposited in the DDBJ/EMBL/GenBank nucleotide sequence databases with the accession numbers AB600751 through AB600834.

Results

Patients' Responses to PEG-IFN/RBV Combination Therapy in HCV-2a and HCV-2b infections

Of the 61 patients infected with HCV-2a, 46 (75%) patients cleared HCV viremia by week 4 (rapid virological response [RVR]), and all the patients (100%) by week 12 (early virological response [EVR]) and at week 24 (end-of-treatment response [ETR]) (Table 1). Likewise, of 51 patients infected with HCV-2b, 34 (67%), 51 (100%) and 50 (98%) patients achieved RVR, EVR and ETR, respectively. After the end of treatment, 105 patients (58 with HCV-2a and 47 with HCV-2b) could be followed up for another 24 weeks. At the end, SVR was achieved by 49 (84%) patients infected with HCV-2a and by 34 (72%) patients with HCV-2b. Only 9 (16%) and 13 (28%) patients with HCV-2a and -2b, respectively, were non-SVR. There was no case of null-response (continuous viremia throughout the treatment and follow up periods) since all the non-SVR patients once cleared viremia at a certain time point followed by a rebound in viremia either before or after the end of the treatment (relapse).

Comparison of the base line demographic characteristics between SVR and non-SVR patients revealed that, in HCV-2a infection, SVR patients had a significantly lower average age than that of non-SVR (Table 2). In HCV-2b infection, on the other hand, SVR patients had significantly γ-GTP levels than those of non-SVR. There was no significant difference in viremia titers between SVR and non-SVR in patients infected with HCV-2a or -2b.

Sequence Analysis of NS5A of HCV-2a and HCV-2b

The entire NS5A region of the HCV-2a and -2b genomes in pretreatment sera were sequenced, and aa sequences deduced. All the sequences obtained were aligned and the consensus sequences for HCV-2a and -2b were inferred. An N-terminal half (aa 1977 to 2196) of the consensus sequences of HCV-2a and -2b isolates were each identical to the prototype sequences, HCV-J6 [18] and

Table 1. Proportions of various virological responses of HCV-2a- and HCV-2b-infected patients treated with PEG-IFN/RBV.

Response	Proportion		
	HCV-2a	HCV-2b	All
RVR	46/61* (75%)	34/51 (67%)	80/112 (71%)
Non-RVR	15/61 (25%)	17/51 (33%)	32/112 (29%)
EVR	61/61 (100%)	51/51 (100%)	112/112 (100%)
ETR	61/61 (100%)	50/51 (98%)	111/112 (99%)
SVR	49/58 (84%)	34/47 (72%)	83/105 (79%)
Non-SVR	9/58 (16%)	13/47 (28%)	22/105 (21%)

*No. of patients/no. of total.
Abbreviations: RVR, rapid virological response; EVR, early virological response; ETR, end-of-treatment response; SVR, sustained virological response.
doi:10.1371/journal.pone.0030513.t001

HCV-J8 [19], respectively. The remaining C-terminal half (aa 2197 to 2442) of the consensus sequences were identical to those reported by Murakami et al. [8] except that His at position 2358 in the HCV-2b sequence was replaced with Cys, which was more conserved (59% of the isolates tested) than His (22%).

To investigate the impact of NS5A heterogeneity on the clinical outcome of PEG-IFN/RBV therapy, we first performed a sliding window analysis with a window size of 20 residues over the full-length NS5A sequences obtained from 23 RVR and 7 non-RVR patients infected with HCV-2a along with the consensus sequence, as described previously [8]. This analysis revealed that the number of aa mutations differed significantly between RVR and non-RVR isolates in two regions within the C-terminal half of NS5A (data not shown). The more C-terminally located one exactly matched the region that corresponded to IRRDR of HCV-1b, ranging from aa 2332 to 2387, thus being referred to as IRRDR[2a] (see Figure 1). The other region composed of a part of ISDR plus its carboxy-flanking region, ranging from aa 2232 to 2262, thus being referred to as ISDR/+C[2a] (see Figure 2). It was confirmed that the average numbers of aa mutations in IRRDR[2a] and ISDR/+C[2a] were each significantly larger in isolates from RVR than those from non-RVR patients (Table 3). More importantly, the average numbers of aa mutations in IRRDR[2a] and ISDR/+C[2a] were each significantly larger in SVR than in non-SVR. Sequences of IRRDR[2a] and ISDR/+C[2a] obtained from SVR and non-SVR patients and the number of mutations of each isolate are shown in Figures 1 and 2.

Likewise, a sliding window analysis on HCV-2b isolates (16 RVR and 6 non-RVR) identified an N-terminal part of IRRDR (aa 2332 to 2357), referred to as IRRDR/N[2b], that showed a significant difference in the number of aa mutations between RVR and non-RVR (data not shown). The average numbers of aa mutations in IRRDR/N[2b] were significantly larger in RVR than in non-RVR (Table 3). However, they did not differ significantly between SVR and non-SVR. Sequences of IRRDR[2b]/N obtained from RVR and non-RVR patients are shown in Figure 3.

Correlation between NS5A Sequence Heterogeneity and SVR or RVR in HCV-2a and HCV-2b infections

The receiver operating characteristic analysis identified the optimal thresholds of the numbers of aa mutations in IRRDR[2a] and ISDR/+C[2a] for the prediction of RVR and SVR in HCV-2a infection; four and one for IRRDR[2a] and ISDR/+C[2a], respectively (data not shown). Accordingly, we found that 86% (42/49) of SVR patients, and only 22% (2/9) of non-SVR, were infected with HCV-2a isolates having IRRDR with 4 or more mutations (IRRDR[2a]≥4) (Table 4). On the other hand, 14% (7/49) of SVR, and 78% (7/9) of non-SVR patients, were infected with isolates having IRRDR with 3 or less mutations (IRRDR[2a]≤3). These results suggested that IRRDR[2a]≥4 was significantly associated with SVR ($P=0.0003$). Similarly, 93% (42/46) of RVR patients, and only 33% (5/15) of non-RVR, were infected with HCV-2a isolates of IRRDR[2a]≥4 while 7% (4/46) of RVR patients, and 67% (10/15) of non-RVR, were infected with HCV-2a isolates of IRRDR[2a]≤3, with the results suggesting that IRRDR[2a]≥4 was significantly associated with RVR as well ($P<0.0001$).

As for ISDR/+C[2a] heterogeneity, 71% (35/49) of SVR, and 22% (2/9) of the non-SVR patients, were infected with HCV-2a isolates with ISDR/+C having one or more mutation (ISDR/+C[2a]≥1) (Table 4). On the other hand, 29% (14/49) of SVR patients, and 78% (7/9) of the non-SVR, were infected with isolates with ISDR/+C without mutation (ISDR/+C[2a] = 0). Thus, ISDR/+C[2a]≥1 was significantly associated with SVR ($P=0.008$).

Table 2. Demographic characteristics of HCV-2a- and HCV-2b-infected patients with SVR and non-SVR.

Factor	HCV-2a			HCV-2b		
	SVR	Non-SVR	*P* value	SVR	Non-SVR	*P* value
Age	49.78±13.67*	62.89±7.01	**0.007**	50.03±15.03	55.08±11.22	0.28
Sex (male/female)	22/27	3/6	0.72	17/17	8/5	0.53
Body weight (kg)	60.39±11.00	54.67±10.51	0.15	57.72±13.46	65.08±7.26	0.06
Platelets ($\times10^4$/mm^3)	18.54±5.71	19.43±10.78	0.72	17.57±5.65	15.20±7.281	0.27
Hemoglobin (g/dl)	14.38±6.07	14.0±1.56	0.88	14.19±1.59	13.78±1.5	0.49
γ-GTP (IU/L)	37.66±53.25	36.83±24.82	0.97	39.68±34.33	81.30±69.11	**0.02**
ALT (IU/L)	64.75±52.45	94.38±141.3	0.28	86.35±91.95	86.85±118.7	0.98
HCV-RNA (KIU/ml)	1350±1424	1598±1464	0.63	5543±7643	7905±14210	0.47
HCV core antigen (fmol/L)	6543±6927	6105±8290	0.91	9054±6743	9390±8723	0.92

*Mean ± S.D.
Abbreviations: SVR, sustained virological response; γ-GTP, gamma glutamyl transpeptidase; ALT, alanine aminotransferase.
doi:10.1371/journal.pone.0030513.t002

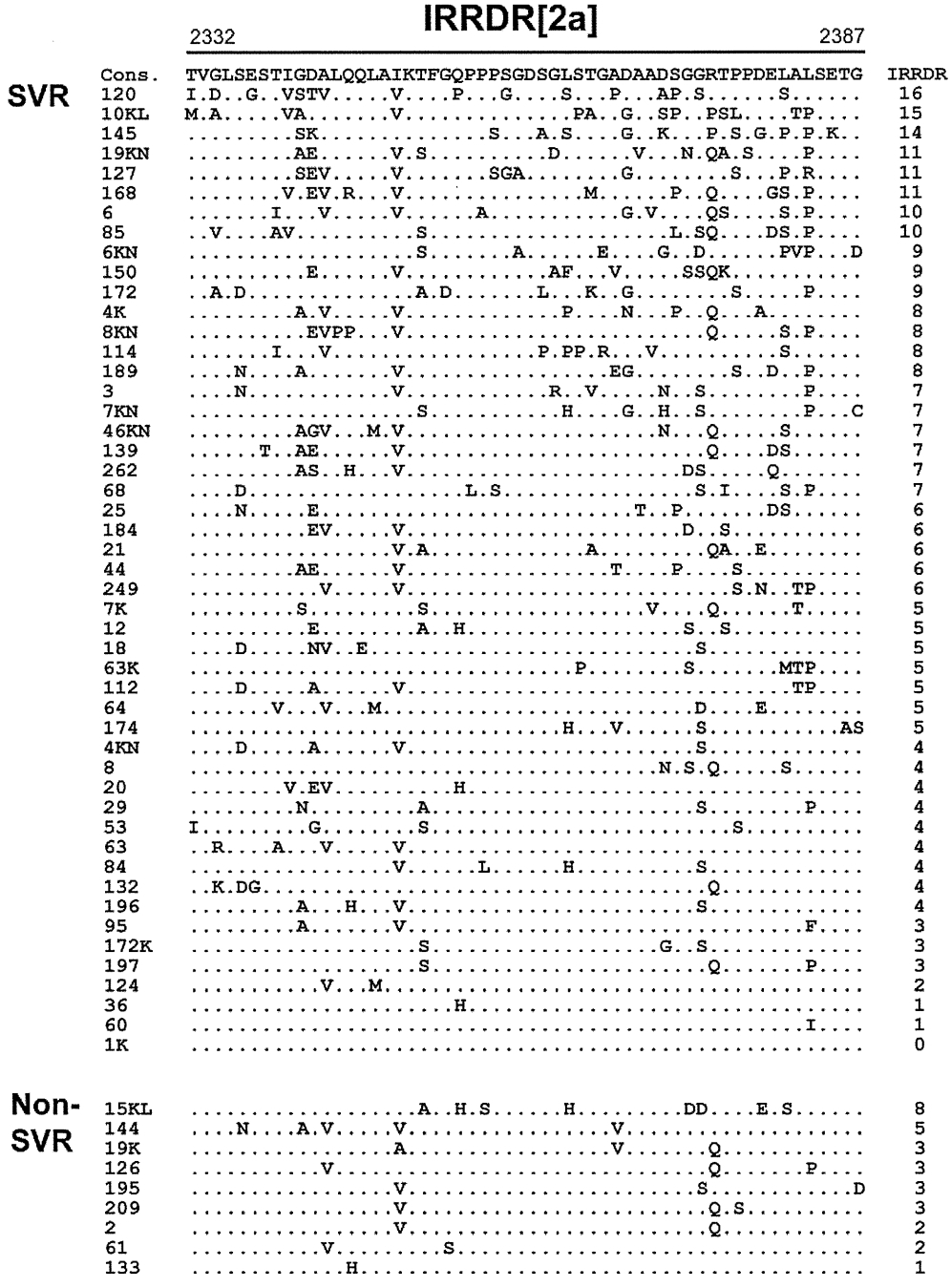

Figure 1. Sequence alignment of IRRDR[2a]. Sequences of IRRDR[2a] (interferon/ribavirin resistance-determining region of HCV-2a) obtained from SVR and non-SVR patients are aligned. The consensus sequence (Cons) is shown on the top. The numbers along the sequence indicate the aa positions. Dots indicate residues identical to those of the Cons sequence. The numbers of the mutations in IRRDR[2a] are shown on the right.
doi:10.1371/journal.pone.0030513.g001

As for HCV-2b infection, the receiver operating characteristic analysis identified "two" as the optimal threshold of the number of mutations in IRRDR/N[2b] by which to predict RVR (data not shown). Accordingly, we found that 65% (22/34) of RVR, and 18% (3/17) of non-RVR patients, were infected with HCV-2b isolates of IRRDR/N[2b]≥2 (Table 4). On the other hand, 35% (12/34) of RVR, and 82% (14/17) of the non-RVR patients, were infected with IRRDR/N[2b]≤1. These results suggested that IRRDR/N[2b]≥2 was significantly associated with RVR ($P = 0.0025$). However, no correlation, or even no tendency toward significant correlation, was observed between IRRDR/N[2b]≥2 and SVR in HCV-2b infection.

Correlation between NS5A Sequence Heterogeneity and Viremia Titers in the Serum of patients infected with HCV-2a and HCV-2b before PEG-IFN/RBV Therapy

Next, we examined the impact of IRRDR sequence heterogeneity on HCV titers in the serum before the initiation of the treatment. As shown in Figure 4A, patients infected with IRRDR[2a]≥4 had significantly lower pretreatment serum

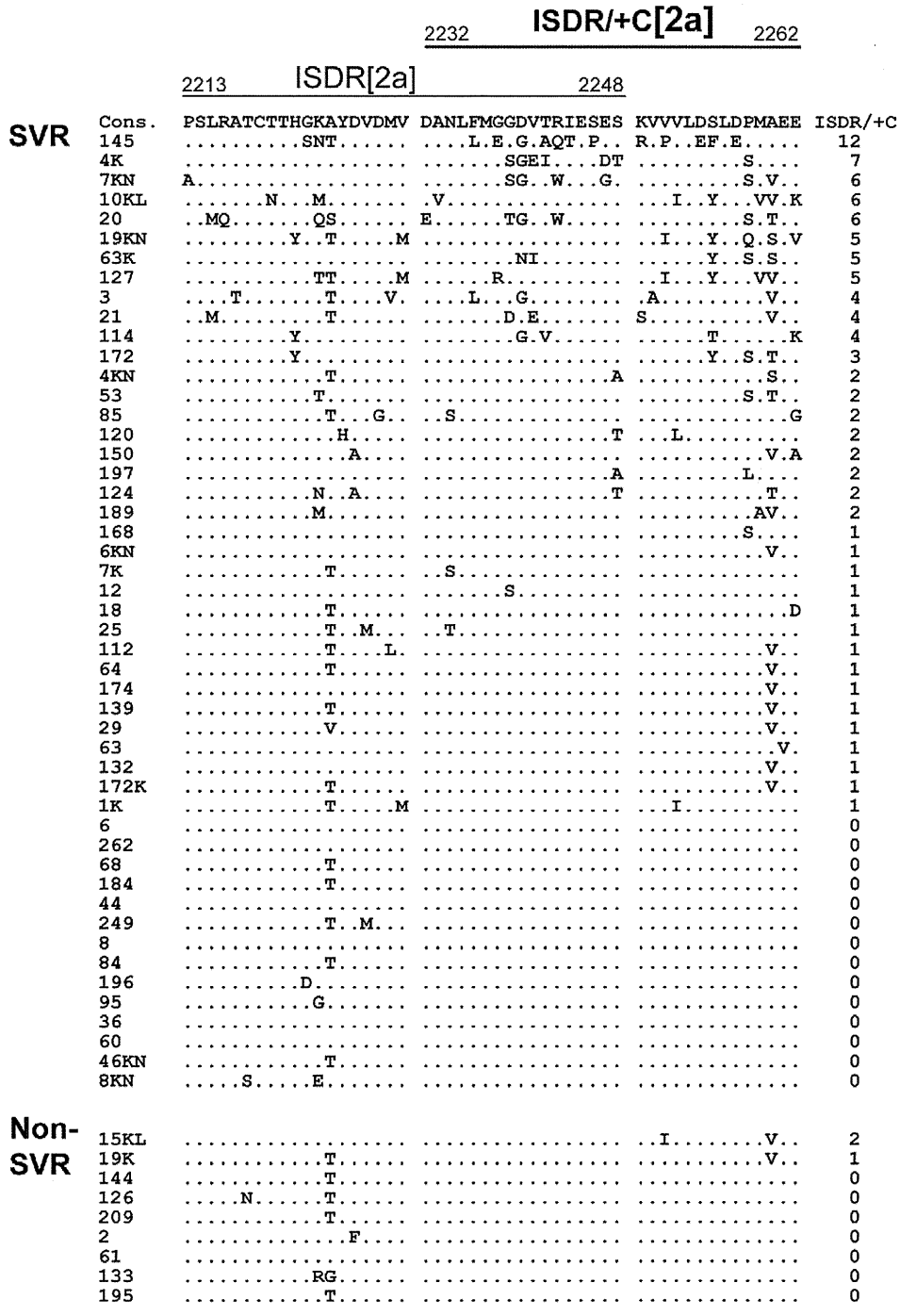

	Cons.	PSLRATCTTHGKAYDVDMV	DANLFMGGDVTRIESES	KVVVLDSLDPMAEE	ISDR/+C
SVR	145	.....SNT.....	....L.E.G.AQT.P..	R.P..EF.E.....	12
	4K	.....	.....SGEI....DT	.....S....	7
	7KN	A.....	.....SG..W...G.	.....S.V..	6
	10KL	.....N...M.....	.V.....	...I..Y...VV.K	6
	20	..MQ.....QS.....	E.....TG..W.....	.....S.T..	6
	19KN	.....Y..T.....M	.....	..I...Y..Q.S.V	5
	63K	.....	.....NI.....	.....Y..S.S..	5
	127	.....TT.....M	.....R.....	..I...Y...VV..	5
	3	....T.....T....V.	....L...G.....	.A.....V..	4
	21	..M.....T.....	.....D.E.....	S.....V..	4
	114	.....Y.....	.....G.V.....	.....T.....K	4
	172	.....Y.....	.....	.....Y..S.T..	3
	4KN	.....T.....	.....A	.....S..	2
	53	.....T.....	.....	.....S.T..	2
	85	.....T...G..	..S.....	.....G	2
	120	.....H.....	.....T	...L.....	2
	150	.....A....	.....	.....V.A	2
	197	.....	.....A	.....L....	2
	124	.....N..A....	.....T	.....T..	2
	189	.....M.....	.....	.....AV..	2
	168	.....	.....	.....S....	1
	6KN	.....	.....	.....V..	1
	7K	.....T.....	..S.....	.....	1
	12	.....	.....S.....	.....	1
	18	.....T.....	.....	.....D	1
	25	.....T..M...	..T.....	.....	1
	112	.....T....L.	.....	.....V..	1
	64	.....T.....	.....	.....V..	1
	174	.....	.....	.....V..	1
	139	.....T.....	.....	.....V..	1
	29	.....V.....	.....	.....V..	1
	63	.....	.....	.....V.	1
	132	.....	.....	.....V..	1
	172K	.....T.....	.....	.....V..	1
	1K	.....T.....M	.....	...I.....	1
	6	.....	.....	.....	0
	262	.....	.....	.....	0
	68	.....T.....	.....	.....	0
	184	.....T.....	.....	.....	0
	44	.....	.....	.....	0
	249	.....T..M...	.....	.....	0
	8	.....	.....	.....	0
	84	.....T.....	.....	.....	0
	196	.....D.....	.....	.....	0
	95	.....G.....	.....	.....	0
	36	.....	.....	.....	0
	60	.....	.....	.....	0
	46KN	.....T.....	.....	.....	0
	8KN	.....S.....E.....	.....	.....	0
Non-SVR	15KL	.....	.....	..I.....V..	2
	19K	.....T.....	.....	.....V..	1
	144	.....T.....	.....	.....	0
	126	.....N.....T.....	.....	.....	0
	209	.....T.....	.....	.....	0
	2	.....F....	.....	.....	0
	61	.....	.....	.....	0
	133	.....RG.....	.....	.....	0
	195	.....T.....	.....	.....	0

Figure 2. Sequence alignment of ISDR/+C[2a]. Sequences of ISDR/+C[2a] (part of interferon sensitivity determining-region plus its carboxy-flanking region of HCV-2a) obtained from SVR and non-SVR patients are aligned. The consensus sequence (Cons) is shown on the top. The numbers along the sequence indicate the aa positions. Dots indicate residues identical to those of the Cons sequence. The numbers of the mutations in ISDR/+C[2a] are shown on the right.
doi:10.1371/journal.pone.0030513.g002

HCV core antigen titers than those infected with IRRDR[2a]≤3. On the other hand, there was no significant difference in HCV viremia titers between ISDR/+C[2a]≥1 and ISDR/+C[2a] = 0 (Figure 4B). Also, in HCV-2b infection, there was no significant difference in pretreatment HCV viremia titers between IRRDR/N[2b]≥2 and IRRDR/N[2b]≤1 (Figure 4C).

Correlation between Core Protein Sequence Heterogeneity and RVR or SVR

A close correlation between core protein sequence patterns and treatment outcome has been proposed in HCV-1b infection [12,13]. To examine this hypothesis in HCV-2a and -2b infections, core regions of the virus genome were amplified from the pretreated sera, and the aa sequences deduced and aligned

Table 3. Average numbers of aa mutations within IRRDR[2a], ISDR/+C[2a] and IRRDR/N[2b] of HCV NS5A obtained form pre-treated sera of HCV-2a and -2b-infected patients with SVR, non-SVR, RVR and non-RVR.

NS5A region	No. of mutations			No. of mutations		
	SVR	Non-SVR	*P* value	RVR	Non-RVR	*P* value
IRRDR[2a] (aa 2332–2387)	6.4±3.4*	3.3±2.1	**0.01**	6.8±3.3	3.3±1.9	0.0003
ISDR/+C[2a] (aa 2232–2262)	2.0±2.4	0.3±0.7	**0.047**	2.1±2.5	0.6±0.7	0.025
IRRDR/N[2b] (aa 2332–2357)	1.8±1.5	1.4±1.3	0.45	2.0±1.4	1.0±1.2	0.01

*Mean ± S.D.

Abbreviations: SVR, sustained virological response; RVR, rapid virological response; IRRDR[2a], interferon/ribavirin resistance-determining region of HCV-2a; ISDR/+C[2a], part of interferon sensitivity determining-region plus its carboxy-flanking region of HCV-2a; IRRDR/N[2b], an N-terminal part of interferon/ribavirin resistance-determining region of HCV-2b.

doi:10.1371/journal.pone.0030513.t003

IRRDR[2b] 2387

2332 **IRRDR/N[2b]** 2357

	Cons.	AKVLTQDNVEGVLREMADKVLSPLQD CNDSGHSTGVDTGGDSVQQPSDETAASEAG	IRRDR/N(2b)	Final response
RVR	73	.....S...I.K.....P.. S....R.....NI...P.....	4	SVR
	138	.....FK...G..F..... H....R...A.....S.	4	SVR
	143	T.....D...R...S... H.....AEA.....TA	4	SVR
	166	.R.....K.....SF.. Y.....A.....D..	4	Non-SVR
	183	.....T...I.K.....P.. S....R.....NI..L...A.V....	4	SVR
	231	.....FN.PR. .....A.....S.D..	4	SVR
	2KL	.....KE.....P.. .....A.....T....	3	SVR
	7	.R.....I.....A..... .....L...A.....D..	3	SVR
	21KN	.....I....VE..... HT.....A.....	3	SVR
	116	.....GE..K..... .....T.	3	SVR
	185	.....I.....I..E. .....A.....D..	3	Non-SVR
	193	.....E...G.....F..... .....A.....T.	3	SVR
	205	.....G....F.....F..... Q.....A.....	3	Non-SVR
	233	.T.....R...K..... .....T.	3	SVR
	4	V.....S..... .Q.....T.	2	Non-SVR
	5KN	.R.....K..... H.....A.....	2	SVR
	9KN	.....K.P.. N....L...AE.....D..	2	SVR
	94	.....F..P.. .....A.....T.	2	SVR
	106K	.....V.....G .D...R.....	2	SVR
	212	.....E.....A..... .....D..	2	SVR
	147	.R.....K..... H.....A.....	2	Unknown
	229	.R.....I.... H.....E.....	2	Non-SVR
	11KL	.....I..... .H.....M.....V..T.	1	SVR
	55KN	.R..... H.....A.....A.....	1	SVR
	87	.....K..... .....T....	1	SVR
	103	..I..... .....AD.....	1	SVR
	165	.....F..... H.....A.....S.	1	SVR
	1K	....A..A....T..T.	0	SVR
	10K	....I.L.....	0	SVR
	46	....	0	SVR
	99	....S..T.	0	SVR
	113	....T...T.	0	SVR
	179	..... H.....A....N.A.....T...S.	0	SVR
	187	..... Y.....T..T.	0	SVR
Non-RVR	18KN	.....G.....F.LP.E .D.....T.	5	SVR
	13K	.....E...K..... .D.....E....K.....	2	Non-SVR
	110	.....H...E..... .H.....N.I..A.....T.	2	Unknown
	11K	.....N..... .....C...A.....C.....G..T.	1	SVR
	23KN	.....E..... .D.....M.....A.....S.	1	Non-SVR
	40KN	.....P.. HS...R.....D.E	1	SVR
	89	.....F..... .....TE	1	Non-SVR
	157	.....N..... YS.....P.....E	1	SVR
	164	.R..... S.....I.....D.....T.	1	SVR
	170	.....E..... SD.....N....I.....T.	1	Unknown
	265KL	.....I..... .....E.	1	Non-SVR
	1	..... YH.....A.....I...P.....	0	Non-SVR
	32KN	....G....	0	Non-SVR
	52	..... H.....A.....T..T.	0	SVR
	105	..... Y.....	0	Non-SVR
	107	.....R.....	0	Non-SVR
	134	....G..T.	0	Unknown

Figure 3. Sequence alignment of NS5A of HCV-2b isolates. Sequences of IRRDR/N[2b] (an N-terminal part of interferon/ribavirin resistance-determining region of HCV-2b) obtained from RVR and non-RVR patients are aligned. The consensus sequence (Cons) is shown on the top. The numbers along the sequence indicate the aa positions. Dots indicate residues identical to those of the Cons sequence. The numbers of the mutations in IRRDR/N[2b] and the final treatment outcome of each patient are shown on the right.

doi:10.1371/journal.pone.0030513.g003